Coupled Physical-Acoustical Data Assimilation in MAB/Shelfbreak PRIMER and First Comparison of the SCS and MAB Frontal Systems

Pierre F.J. Lermusiaux, Allan R. Robinson, Ching-Sang Chiu (NPS),

Patrick J. Haley and Wayne G. Leslie

Division of Engineering and Applied Sciences

Department of Earth and Planetary Sciences

http://www.deas.harvard.edu/~pierrel

http://www.deas.harvard.edu/~robinson

Table of Contents

PHYSICAL-ACOUSTICAL FILTERING IN A SHELFBREAK ENVIRONMENT:

Ocean Physics as Simulated 2 Years Ago

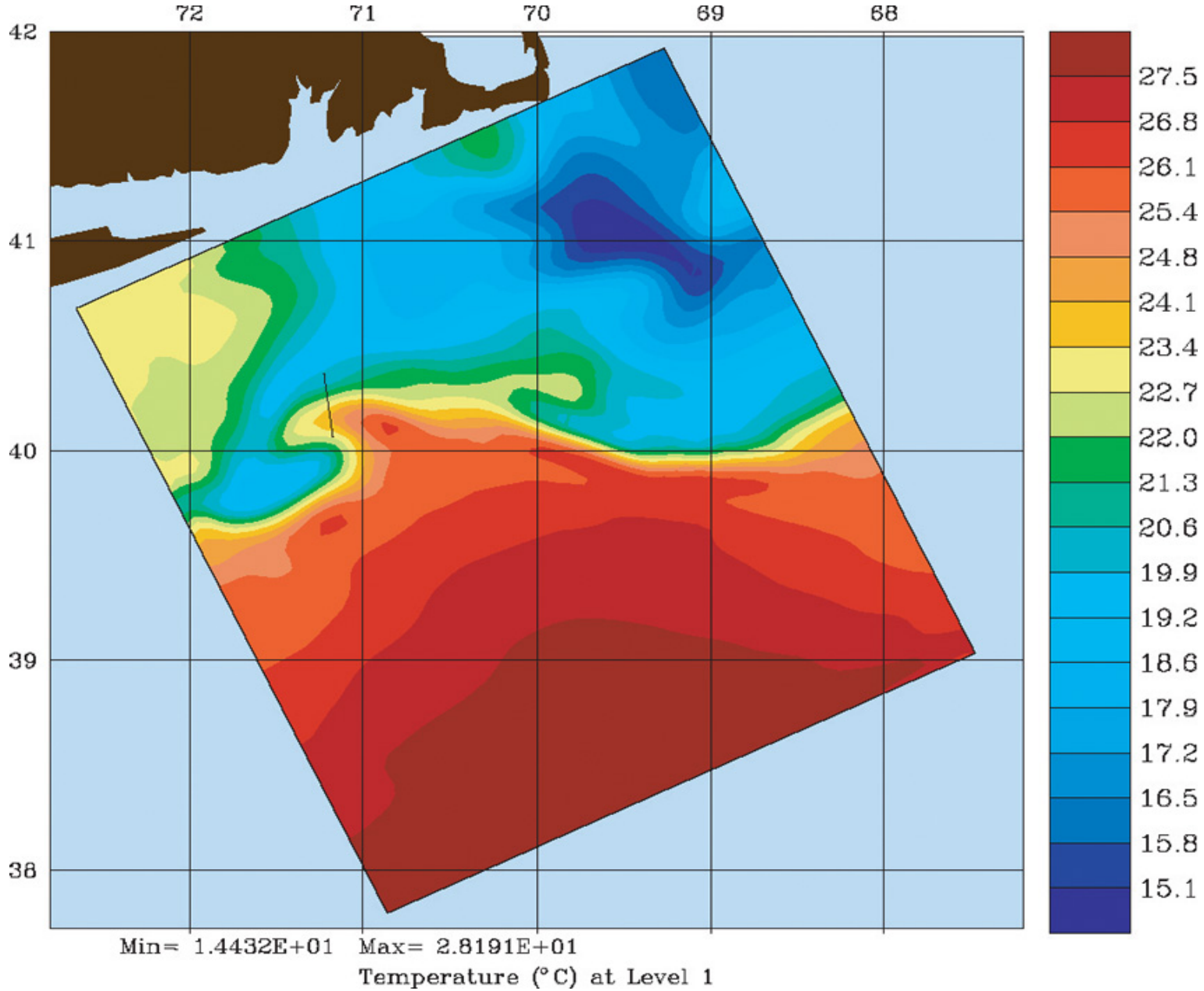

30m Temperature as Simulated in June 04

July 18, 1996

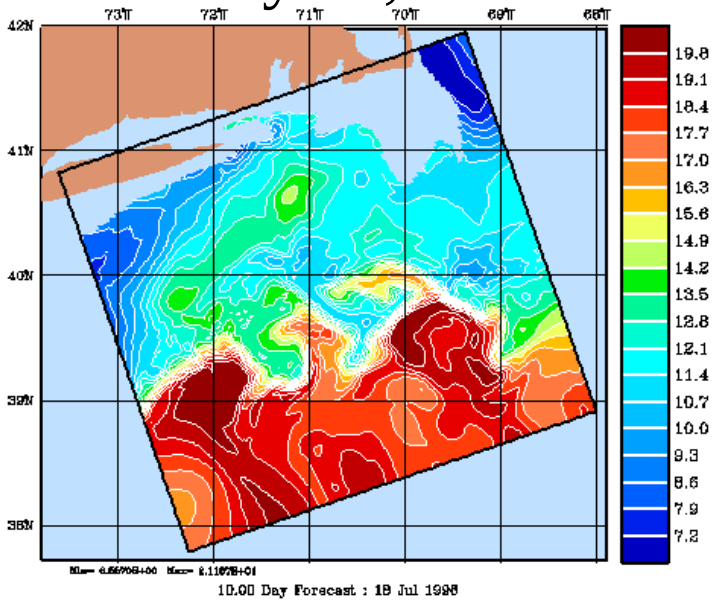

July 20, 1996

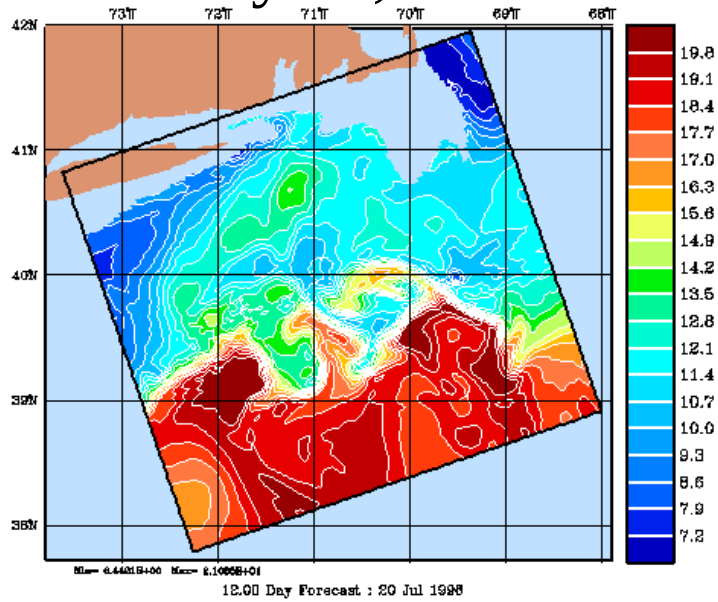

July 22, 1996

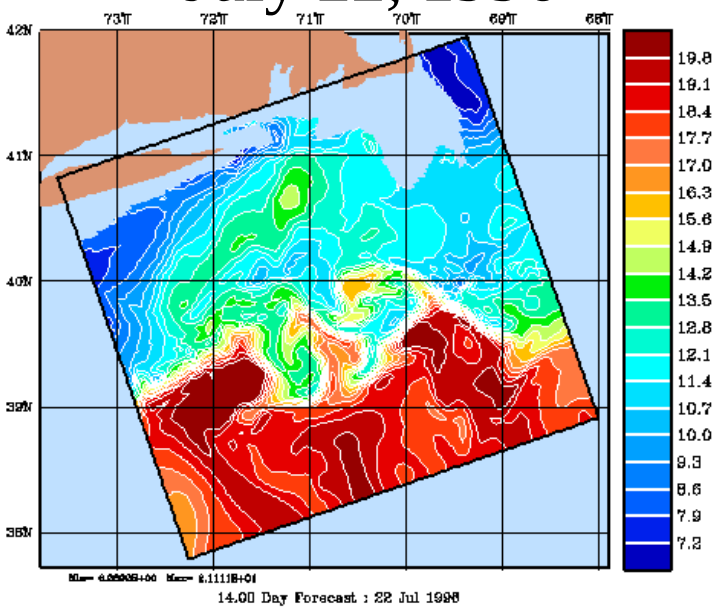

July 26, 1996

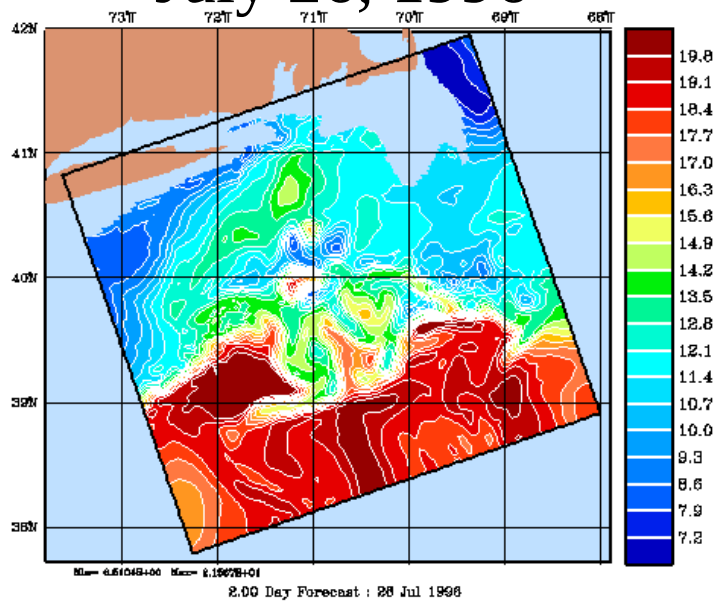

Evaluation based on SST

July 18

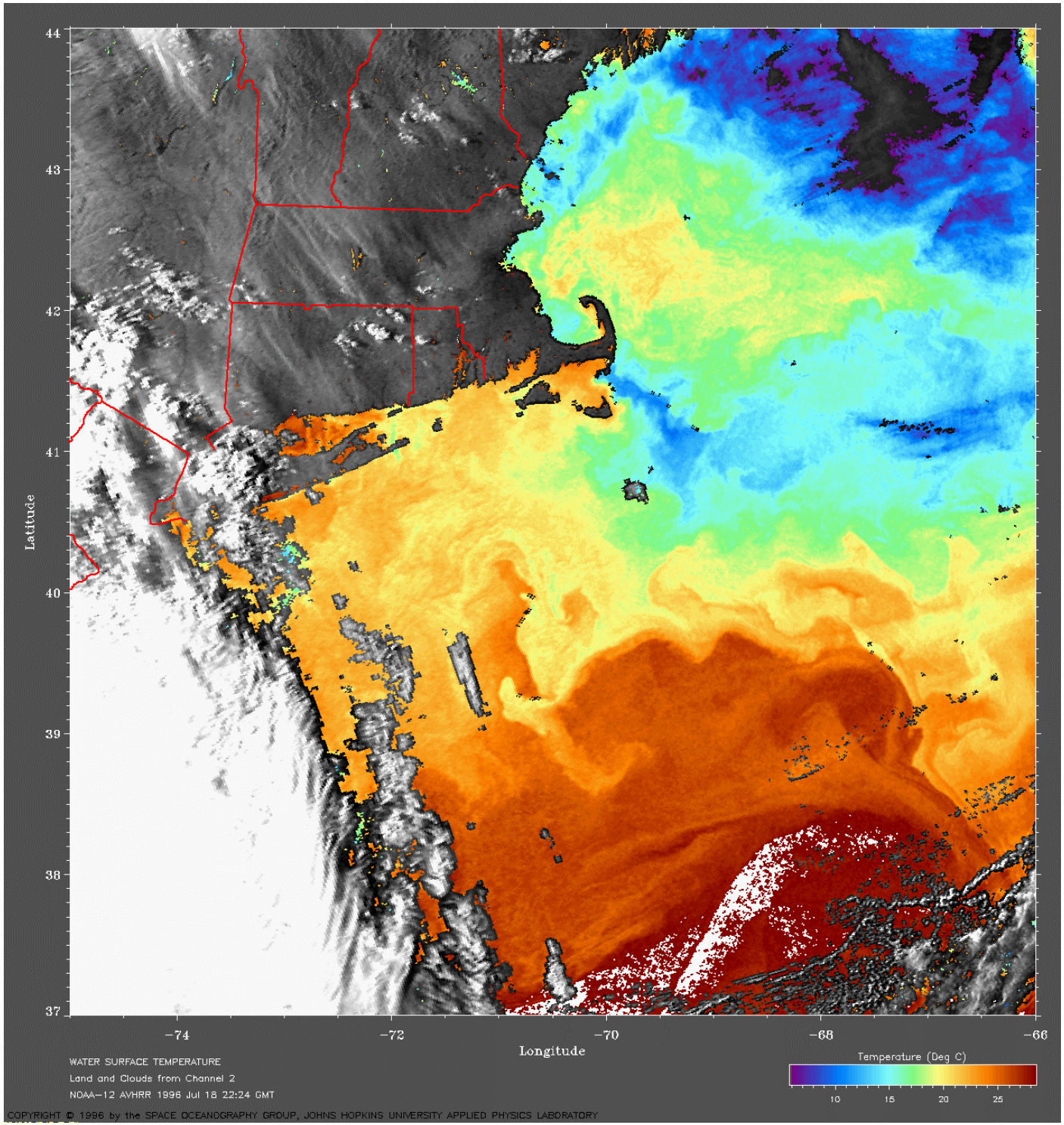

Evaluation based on SST

July 20

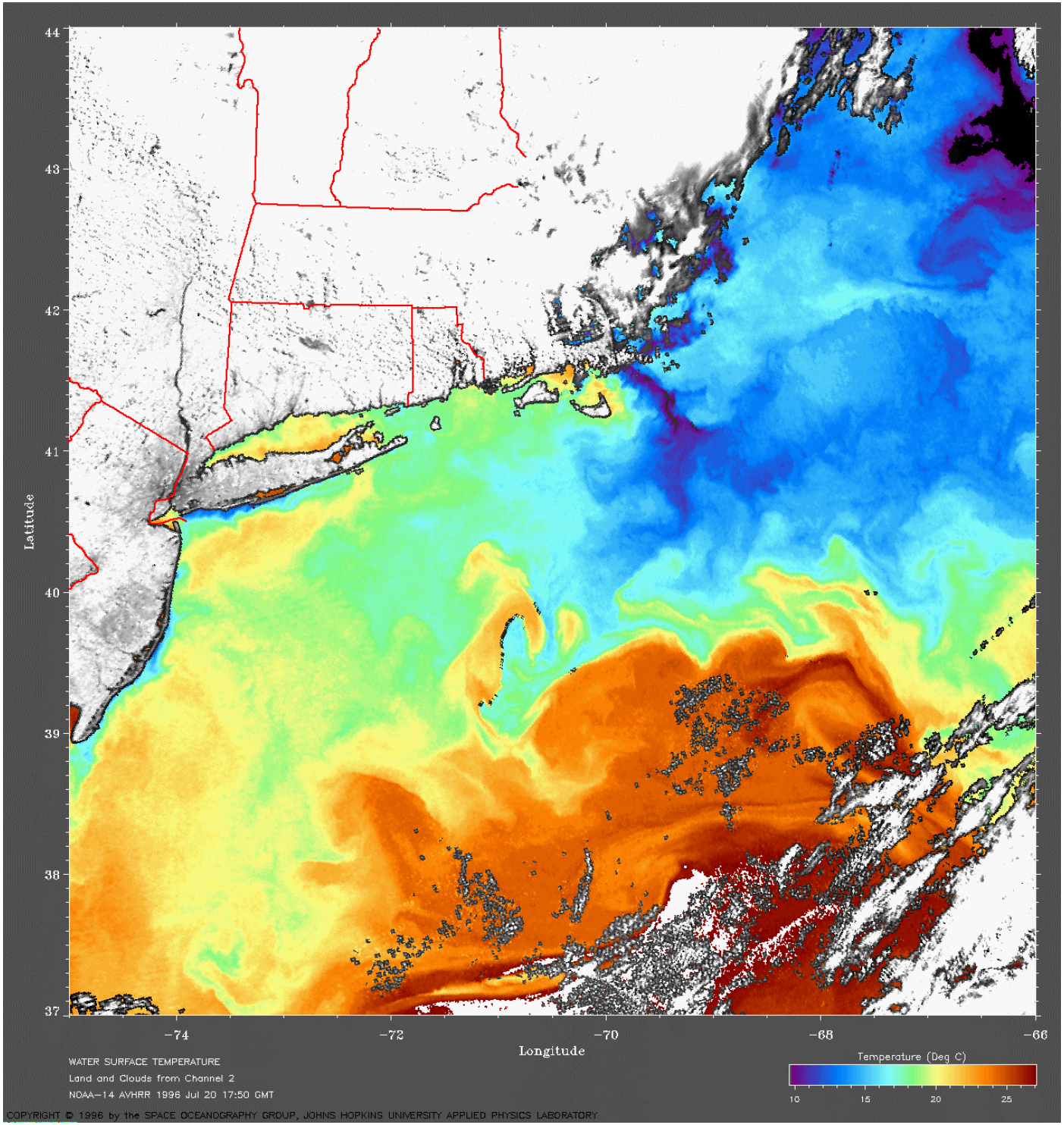

Evaluation based on SST

July 22

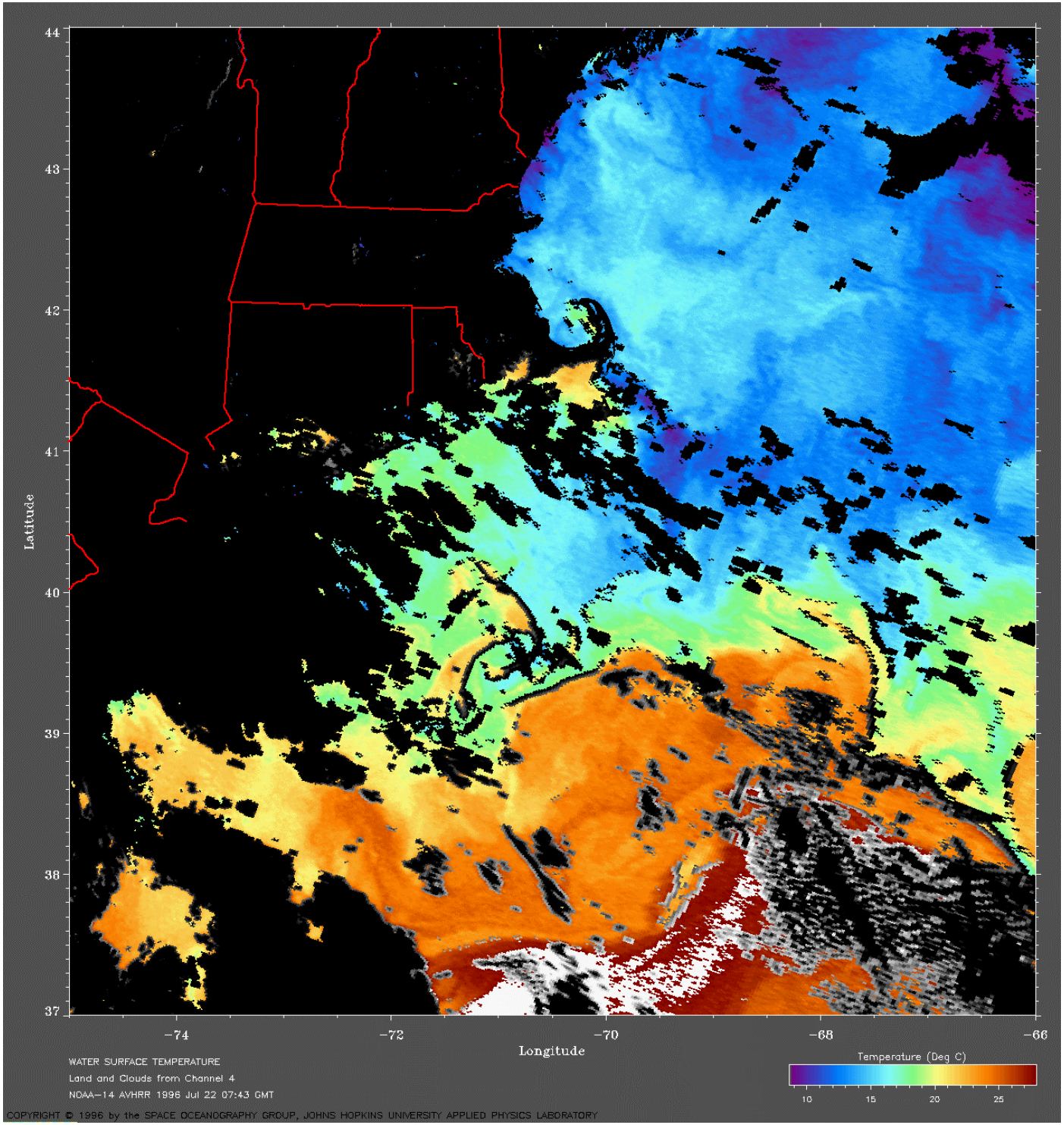

30m Temperature: 8 July – 7 August 1996

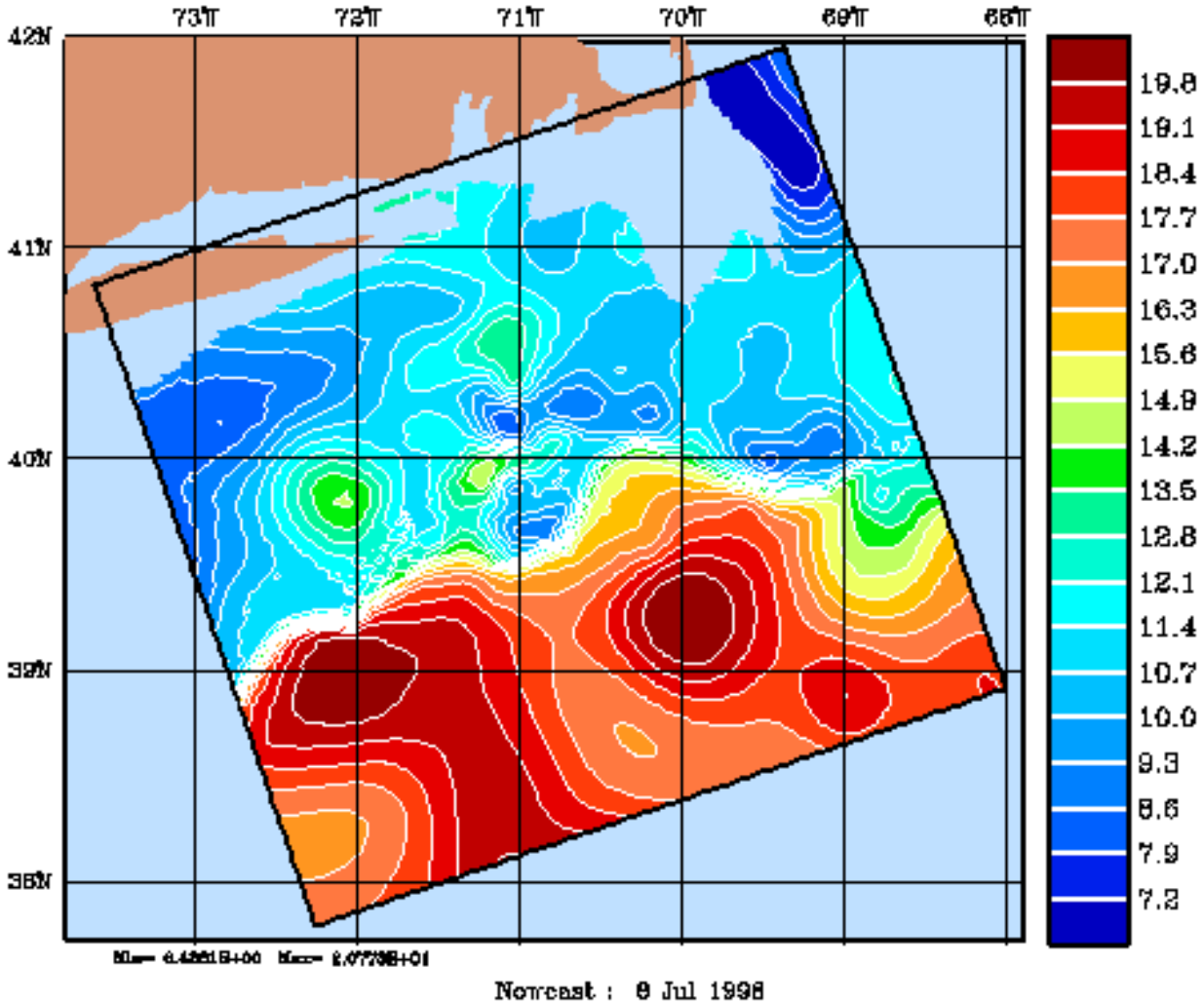

Importance and Effects of Atmospheric Forcings and Uncertainties

Best Run

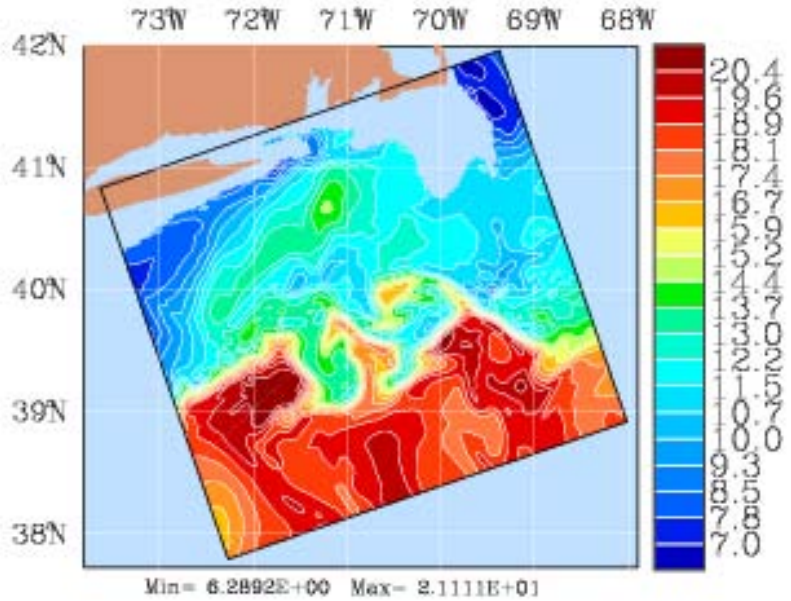

No Atmos. Forcing

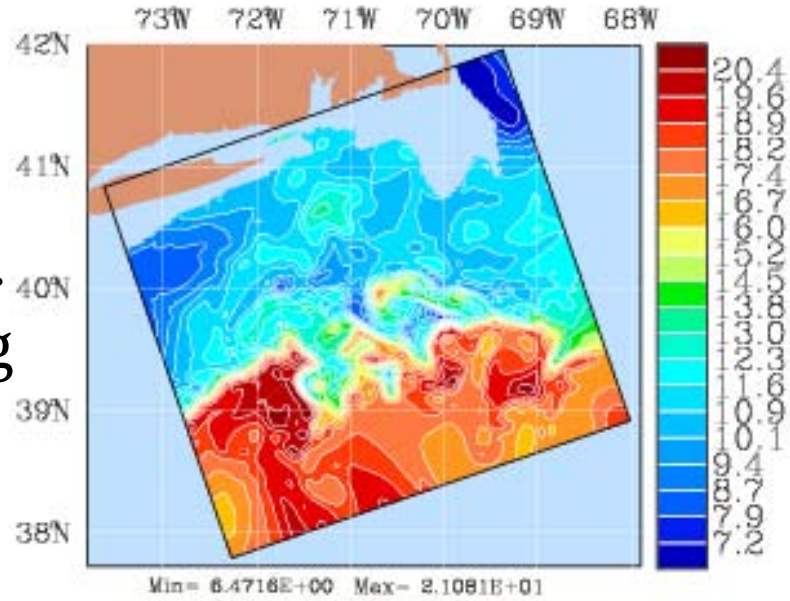

Too strong transfer of atmos. forcing

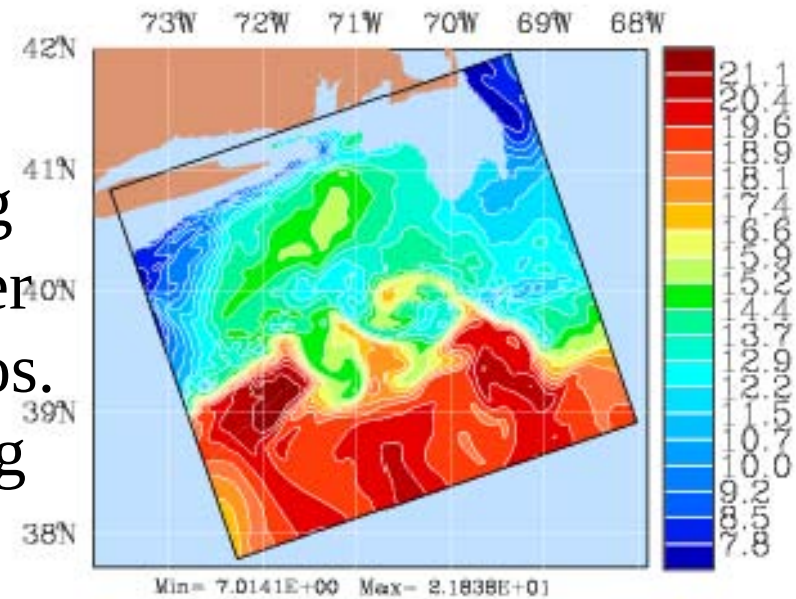

- Oceanic frontal instabilities occur from sub-mesoscales to mesoscales
- Atmospheric forcing impose certain scales on multi-scale oceanic frontal instability
- Deeper surface boundary layer and increased SBL mixing deepens large frontal meander but does not lead to much stronger surface signal

Quick-Look evaluations of 50m Temperature: July 26, 1996

Gawarkiewicz, et al. 50m potential temperature for 26 July, 29 July and 31 July, objectively analyzed from Seasoar data

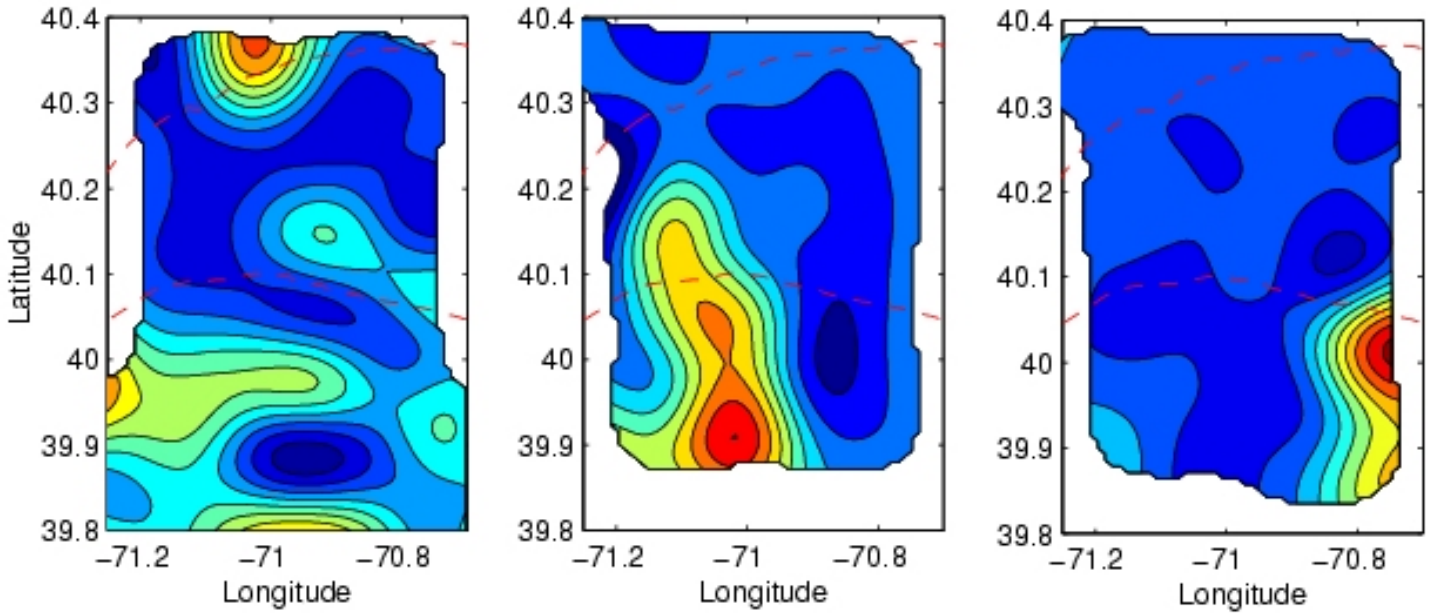

50m temperature in HOPS simulation with data assimilation for the same dates

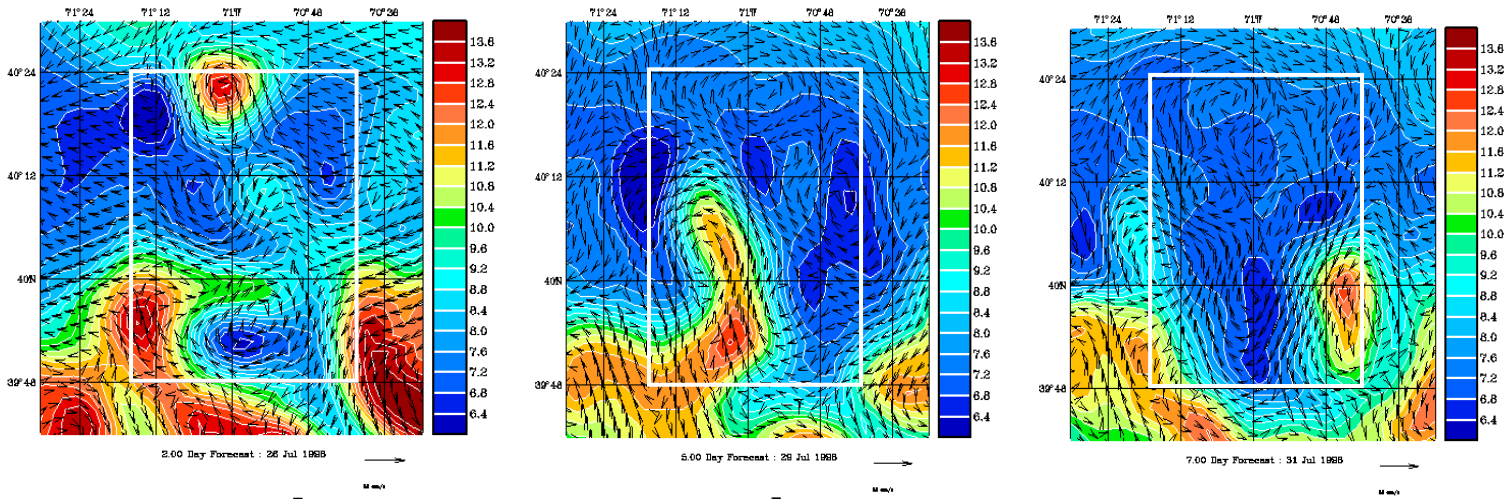

26 July 29 July 31 July

50m Temperature: 8 July – 7 August 1996

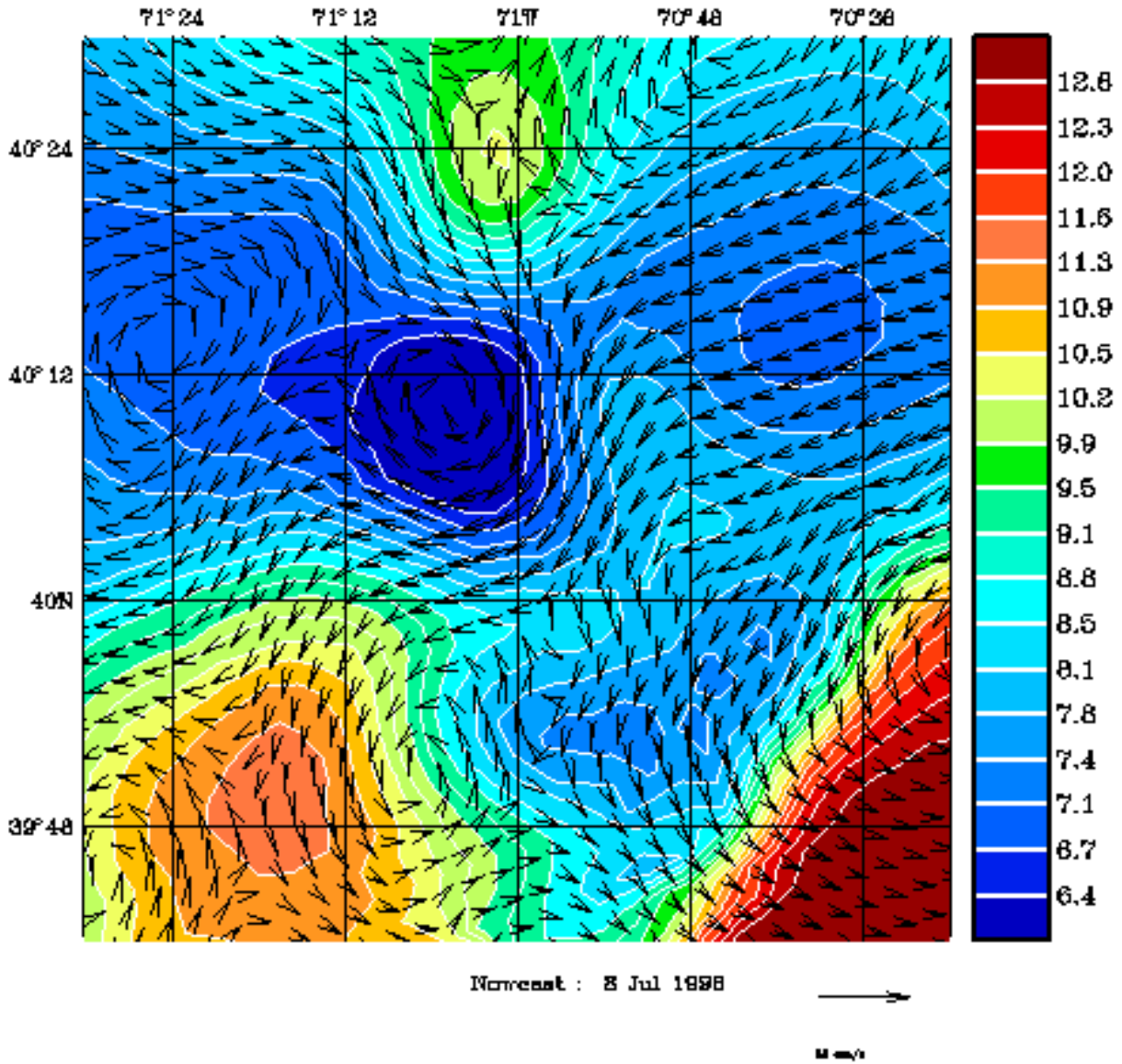

50m Temperature: July 26, 1996

No DA

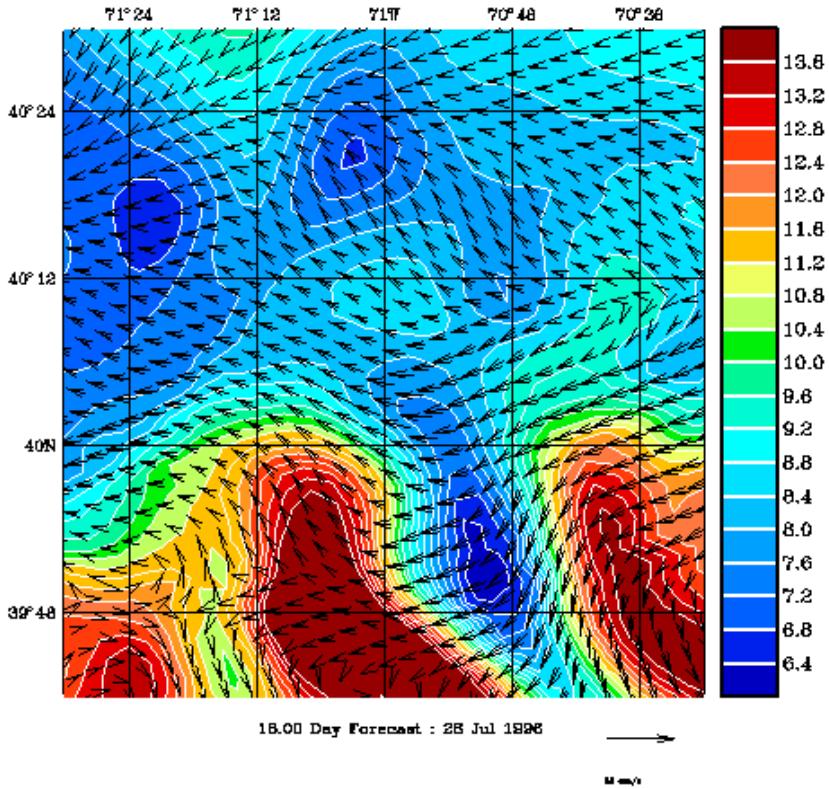

18 day predictions

With DA

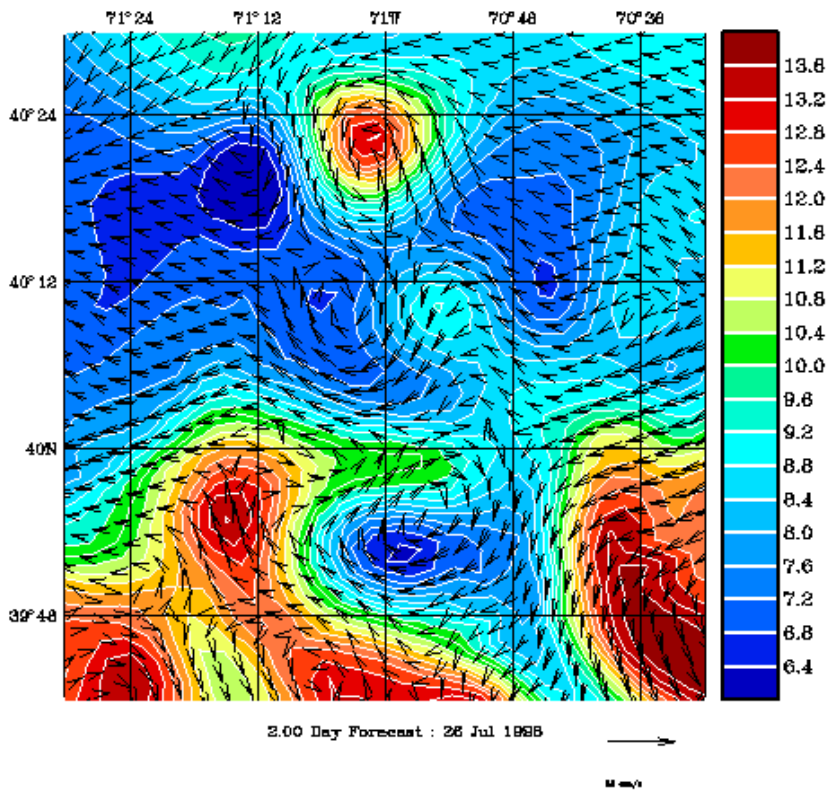

18 day predictions, with DA of July 26 data

ESSE: Uncertainty Predictions and Data Assimilation

1. Dynamics: $dx = M(x)dt + d\eta$ $\quad \eta \sim N(0, Q)$
2. Measurement: $y = H(x) + \varepsilon$ $\quad \varepsilon \sim N(0, R)$

3. Non-lin. Err. Cov. evolution: $P(0)=P_0$

$$dP/dt = <(x-\hat{x})(M(x)-M(\hat{x}))^T> + <(M(x)-M(\hat{x})(x-\hat{x})^T> + Q$$

4. Error reduction by DA:

$P(+) = (I - KH)P(-)$ where K is the reduced Kalman Gain

- ESSE retains and nonlinearly evolves uncertainties that matter, combining,
  - i. Proper Orthogonal Decompositions (PODs) or Karhunen-Loeve (KL) expansions

$$\mathbf{u} = \sum_{i=1}^{M} \phi_{\mathbf{u}}(x,y,z)\, \mathbf{a}_i(t) \quad \rightarrow \quad \frac{d\,\mathbf{a}_i(t)}{dt} = \mathbf{f}(\mathbf{a})$$

  - ii. Time-varying basis functions, and,
  - iii. Multi-scale initialisation and Stochastic ensemble predictions

  to obtain a dynamic low-dimensional representation of the error space.

- Linked to Polynomial chaos, but with time-varying error KL basis:

$$\mathbf{x}(x,t,\theta) = \bar{\mathbf{x}}(x,t) + \sum_{i=1}^{M} \sqrt{\lambda_i}\ \phi_u^s(\mathbf{x},t)\, \zeta_i(\theta)$$

Sources of Uncertainty in Simulations of Ocean Physics

- Bathymetry
- Boundary conditions
  - Surface atmospheric forcing
  - Coastal-estuary and open-boundary fluxes
- Initial conditions
- Ocean physics data
- Model parameters and parameterized processes: sub-grid-scales, turbulence closures, un-resolved processes
  - e.g. tides and internal tides, internal waves and solitons, microstructure and turbulence
- Numerical errors: steep topographies/pressure gradient, non-convergence

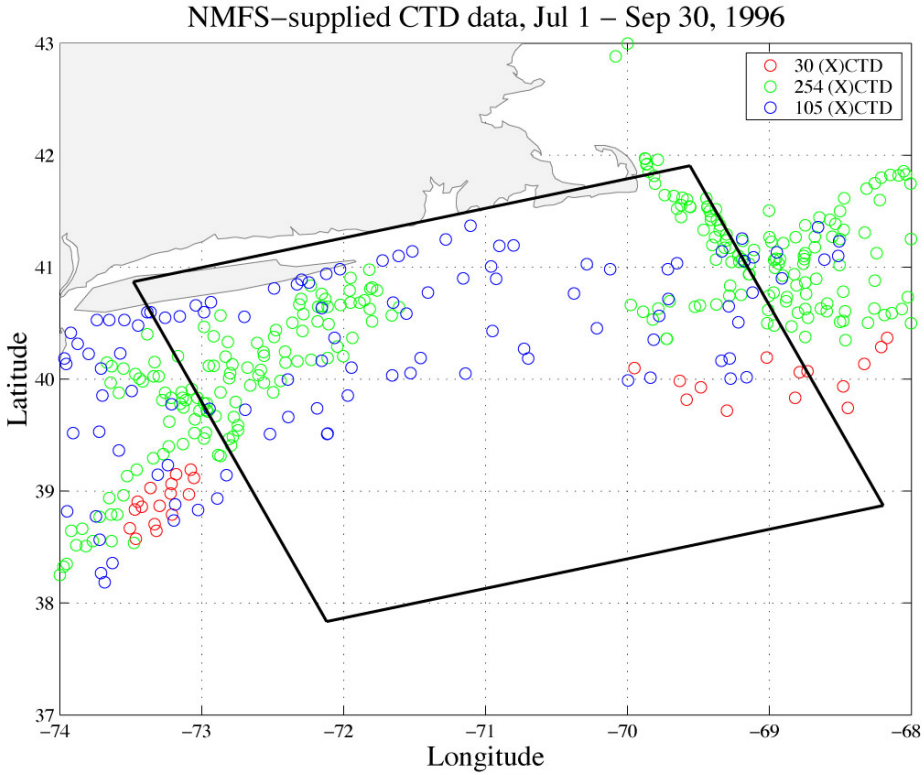
NMFS−supplied CTD data, Jul 1 − Sep 30, 1996
30 (X)CTD
254 (X)CTD
105 (X)CTD
Latitude
Longitude

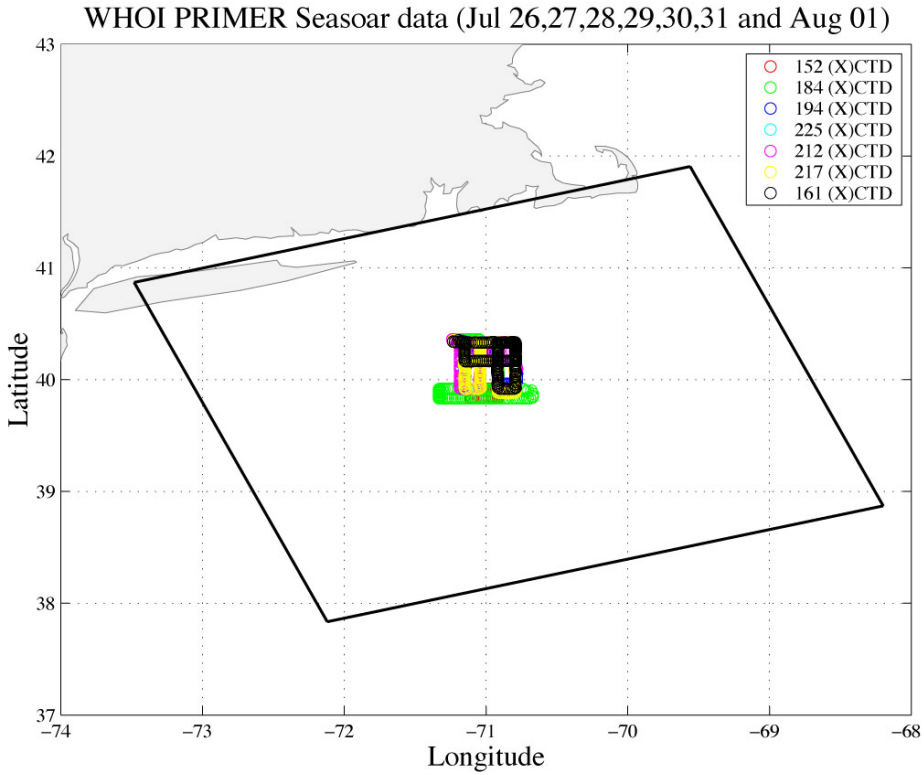
WHOI PRIMER Seasoar data (Jul 26,27,28,29,30,31 and Aug 01)
152 (X)CTD
184 (X)CTD
194 (X)CTD
225 (X)CTD
212 (X)CTD
217 (X)CTD
161 (X)CTD
Latitude
Longitude

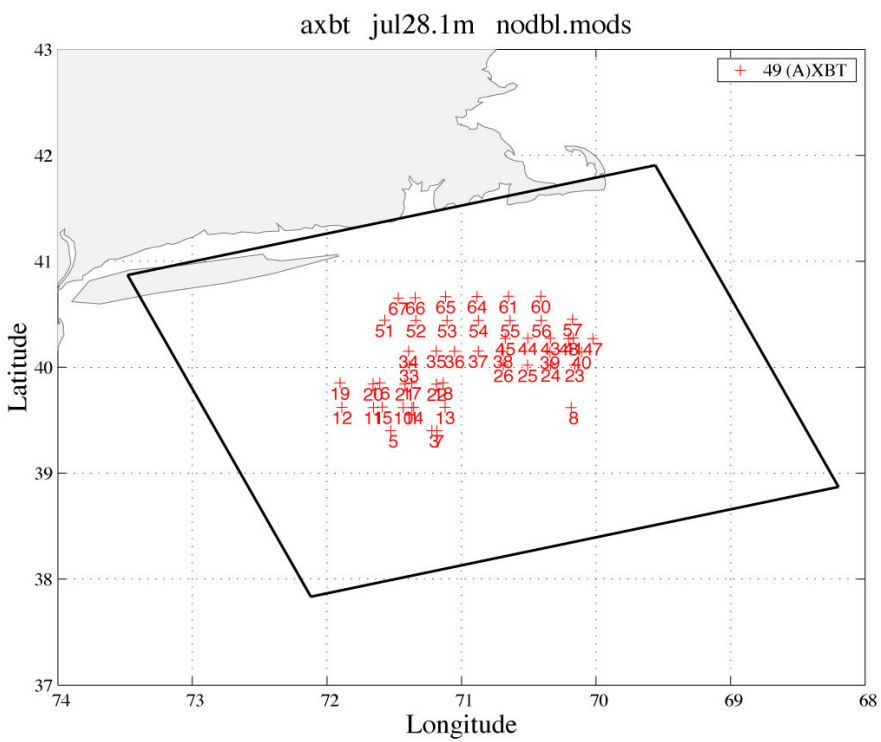
axbt jul28.1m nodbl.mods
49 (A)XBT
Latitude
Longitude

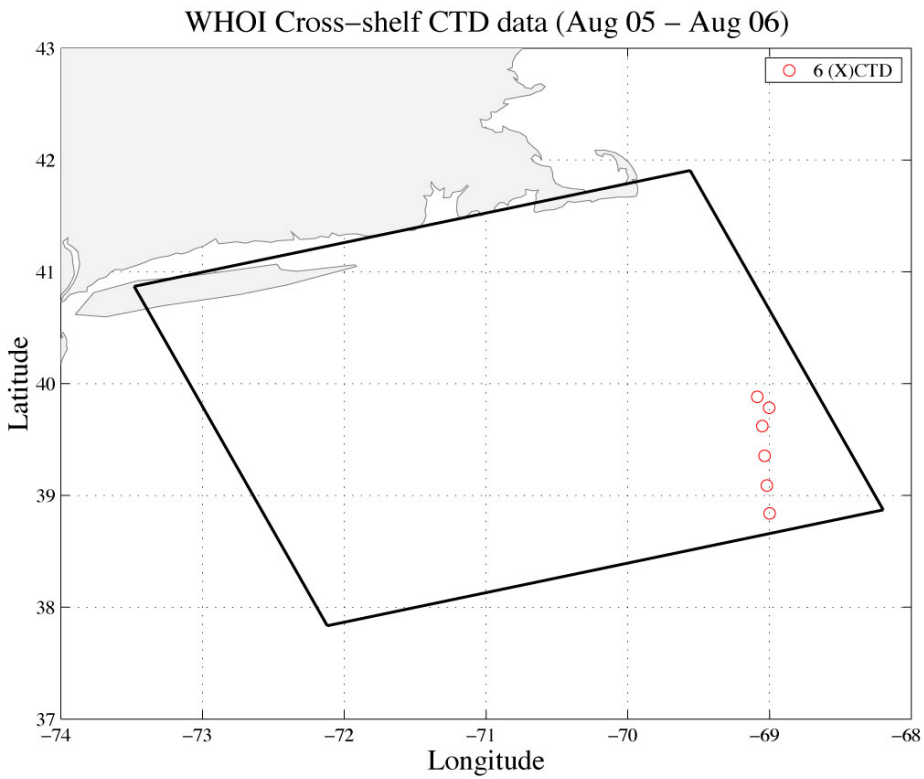
WHOI Cross−shelf CTD data (Aug 05 − Aug 06)
6 (X)CTD
Latitude
Longitude

Initial condition uncertainties: Positions and shapes of the tilted shelfbreak front

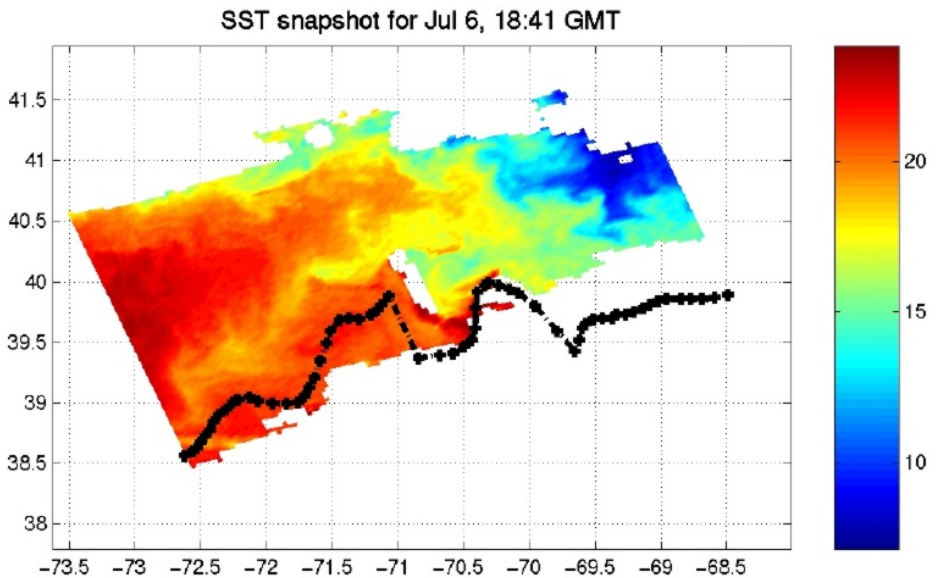

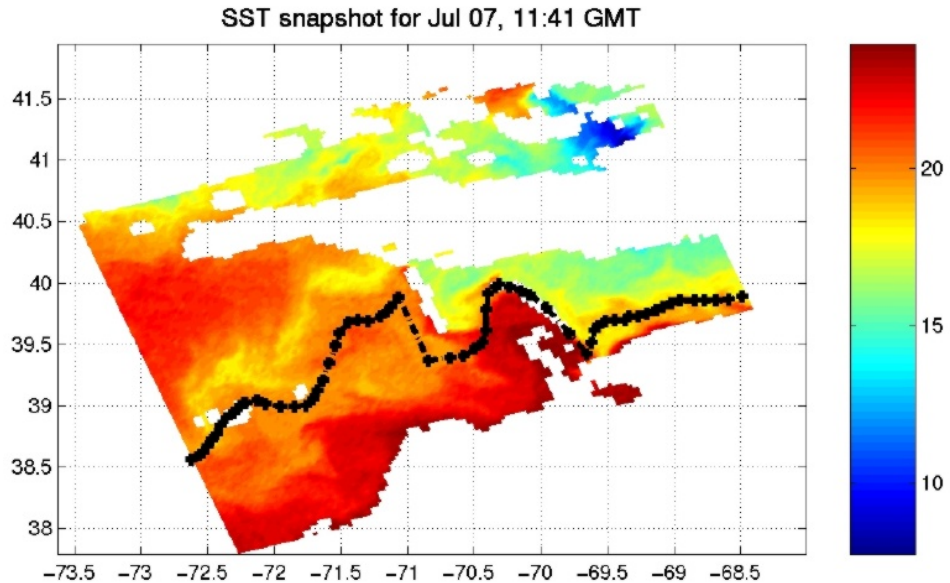

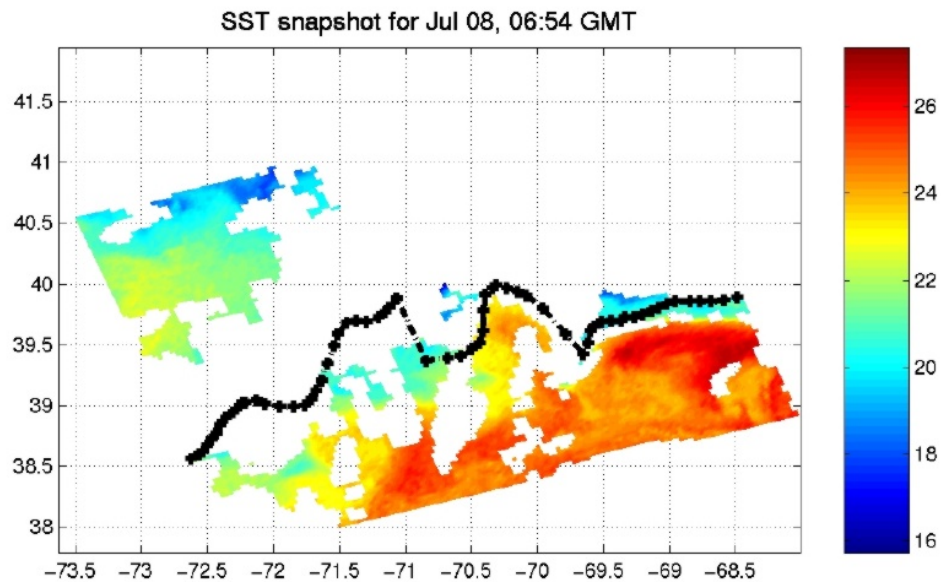

Outcropping of surface front

- Upstream positions relatively certain, with sharp ring-front interactions
- Downstream positions very uncertain:
  - Notice surface signature of advected shelf waters
  - SBF meandering and “old” weak warm core rings
  - Squirts of slope and shelf waters

IC uncertainties: Positions and shapes of the tilted SBF (cont.)

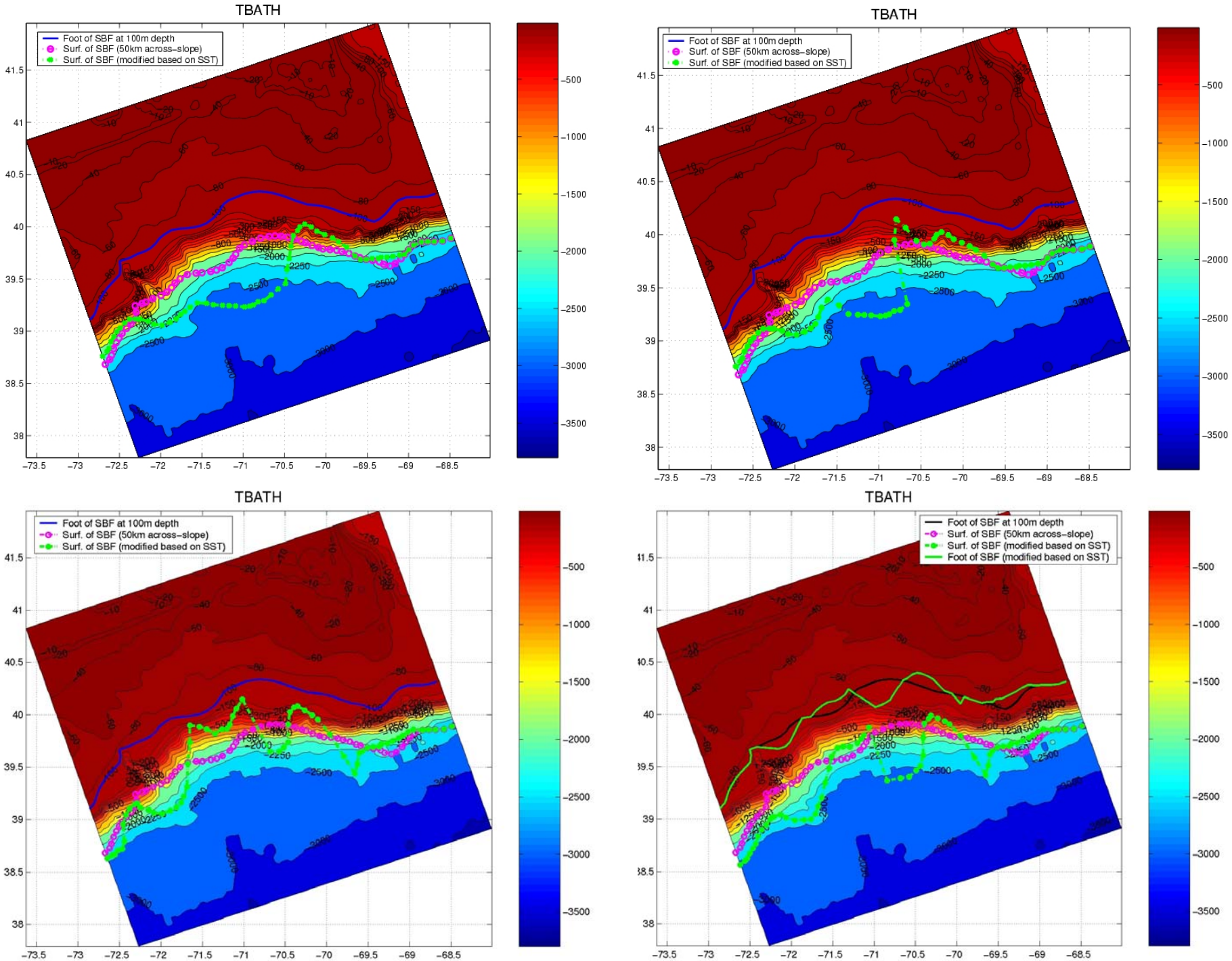

Uncertainties in Multiple Model Parameters: Example of mixing layer depth (Ekman factor E_k)

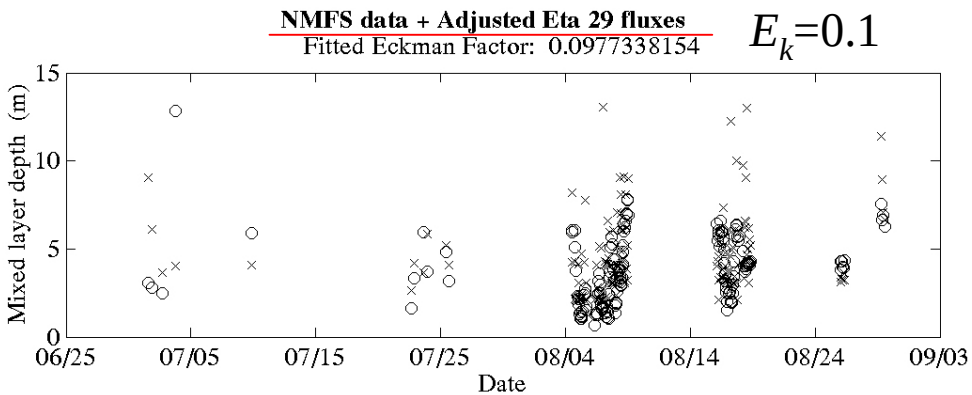

day

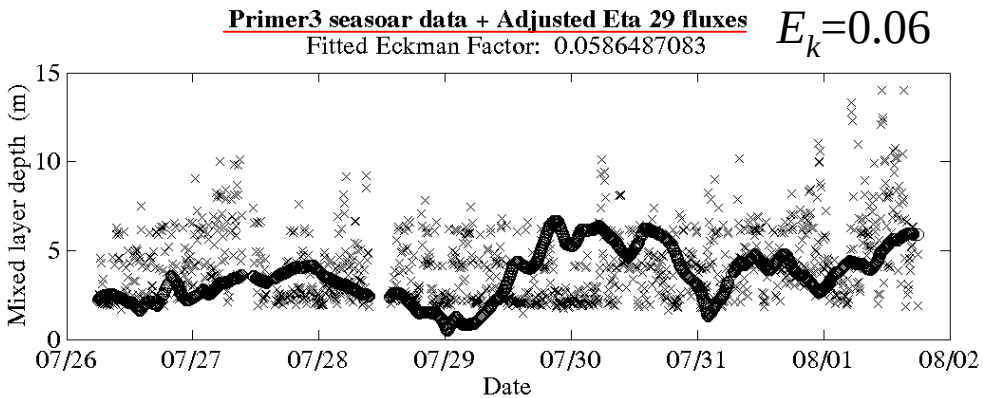

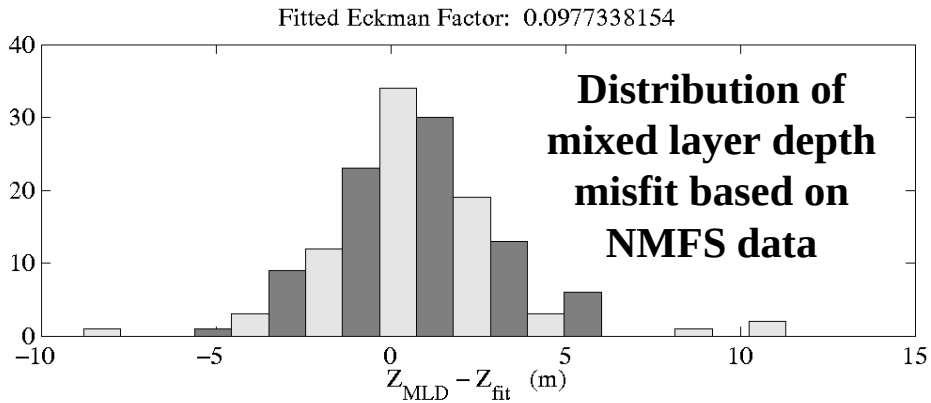

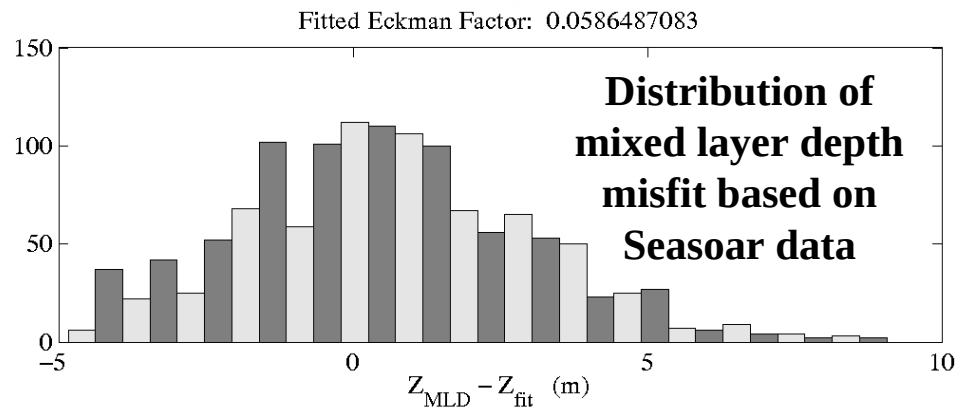

- Similar uncertainties and fit for several other parameters
- Need for adaptive modeling (e.g. parameter values that evolve in time as a function of data)
- One reason: (sub)-mesocale coastal variabilities and atmosphere-ocean interactions are not stationary at scales of days to a month

Stochastic Primitive Equation Model

The diagonal of time-decorrelations:

β_u, β_v, β_T, β_S, β_ψ **functions of** (x, y, z)

are here chosen $\beta_X = \beta \mathbf{I}$.

The diagonal of noise variances are chosen function of z only, of amplitude set to: "ε * geostrophy"

$$\boldsymbol{\Sigma}_u = \boldsymbol{\Sigma}_v = \sigma^2(z)\,\mathbf{I}\ , \quad \text{with } \sigma_U(z) = \epsilon_U\, f_c\, U(z)\ ,$$

$$\boldsymbol{\Sigma}_T = \sigma_T^2(z)\,\mathbf{I}\ , \quad \text{with } \sigma_T(z) = \epsilon_T\, U(z)\, \frac{\Delta T(z)}{L(z)}\ ,$$

$$\boldsymbol{\Sigma}_S = \sigma_S^2(z)\,\mathbf{I}\ , \quad \text{with } \sigma_S(z) = \epsilon_S\, U(z)\, \frac{\Delta S(z)}{L(z)}\ ,$$

$$\boldsymbol{\Sigma}_\psi = \sigma_\psi^2(z)\,\mathbf{I}\ , \quad \text{with } \sigma_\psi(z) = \epsilon_\psi\, \frac{\overline{\omega}\, L(z)}{U(z)}\ ,$$

Internal Baroclinic Zonal Mode

$$\mathbf{d\hat{u}} = \mathbf{du'} - \mathbf{d\overline{u}'}\ , \tag{82a}$$

$$\mathbf{du'} = \left(-\boldsymbol{\Gamma}(\mathbf{u}) + \mathbf{fv} - \frac{\mathbf{g}}{\boldsymbol{\rho}_0}\int_\mathbf{z}^0 \boldsymbol{\rho}_\mathbf{x}\, \mathbf{dz} + \mathbf{F}_u + \mathbf{A}_v \mathbf{u}_\mathbf{zz}\right) dt + \mathbf{B}_u^{fc}\, \mathbf{d\tilde{w}}_u^c\ ,$$

$$\text{with}\quad \mathbf{u} = \hat{\mathbf{u}} - \tfrac{1}{\mathbf{H}}\boldsymbol{\psi}_\mathbf{y}\ .$$

$$\mathbf{d\tilde{w}}_u^c = -\boldsymbol{\beta}_u\, \tilde{\mathbf{w}}_u^c\, dt + \mathbf{dw}_u^c\ , \tag{82b}$$

$$\text{with}\quad \tilde{\mathbf{w}}_u^c(0) \sim (\mathbf{0}, \boldsymbol{\Sigma}_u)\quad \text{and}\quad \mathbf{w}_u^c \sim (\mathbf{0}, 2\boldsymbol{\beta}_u \boldsymbol{\Sigma}_u)\ .$$

Internal Baroclinic Meridional Mode

$$\mathbf{d\hat{v}} = \mathbf{dv'} - \mathbf{d\overline{v}'}\ , \tag{82c}$$

$$\mathbf{dv}_t' = \left(-\boldsymbol{\Gamma}(\mathbf{v}) - \mathbf{fu} - \frac{\mathbf{g}}{\boldsymbol{\rho}_0}\int_\mathbf{z}^0 \boldsymbol{\rho}_y\, \mathbf{dz} + \mathbf{F}_v + \mathbf{A}_v \mathbf{v}_\mathbf{zz}\right) dt + \mathbf{B}_v^{fc}\, \mathbf{d\tilde{w}}_v^c\ ,$$

$$\text{with}\quad \mathbf{v} = \hat{\mathbf{v}} + \tfrac{1}{\mathbf{H}}\boldsymbol{\psi}_\mathbf{x}\ .$$

$$\mathbf{d\tilde{w}}_v^c = -\boldsymbol{\beta}_v\, \tilde{\mathbf{w}}_v^c\, dt + \mathbf{dw}_v^c\ , \tag{82d}$$

$$\text{with}\quad \tilde{\mathbf{w}}_v^c(0) \sim (\mathbf{0}, \boldsymbol{\Sigma}_v)\quad \text{and}\quad \mathbf{w}_v^c \sim (\mathbf{0}, 2\boldsymbol{\beta}_v \boldsymbol{\Sigma}_v)\ .$$

Thermal energy: Balance

$$\mathbf{dT} = \left(-\boldsymbol{\Gamma}(\mathbf{T}) + \mathbf{F}_T + \mathbf{K}_v \mathbf{T}_\mathbf{zz}\right) dt + \mathbf{B}_T^{fc}\, \mathbf{d\tilde{w}}_T^c\ , \tag{82e}$$

$$\mathbf{d\tilde{w}}_T^c = -\boldsymbol{\beta}_T\, \tilde{\mathbf{w}}_T^c\, dt + \mathbf{dw}_T^c\ , \tag{82f}$$

$$\text{with}\quad \tilde{\mathbf{w}}_T^c(0) \sim (\mathbf{0}, \boldsymbol{\Sigma}_T)\quad \text{and}\quad \mathbf{w}_T^c \sim (\mathbf{0}, 2\boldsymbol{\beta}_T \boldsymbol{\Sigma}_T)\ .$$

Conservation : of Salt

$$\mathbf{dS} = \left(-\boldsymbol{\Gamma}(\mathbf{S}) + \mathbf{F}_S + \mathbf{K}_v \mathbf{S}_\mathbf{zz}\right) dt + \mathbf{B}_S^{fc}\, \mathbf{d\tilde{w}}_S^c\ , \tag{82g}$$

$$\mathbf{d\tilde{w}}_S^c = -\boldsymbol{\beta}_S\, \tilde{\mathbf{w}}_S^c\, dt + \mathbf{dw}_S^c\ , \tag{82h}$$

$$\text{with}\quad \tilde{\mathbf{w}}_S^c(0) \sim (\mathbf{0}, \boldsymbol{\Sigma}_S)\quad \text{and}\quad \mathbf{w}_\psi^c \sim (\mathbf{0}, 2\boldsymbol{\beta}_\psi \boldsymbol{\Sigma}_S)\ .$$

Barotropic Stream Function

$$\nabla_h \wedge [\mathbf{H}^{-1}\nabla_\mathbf{h} \wedge \mathbf{d}\boldsymbol{\psi}\, \mathbf{e}_3] = -\nabla_h \wedge \mathbf{d\overline{u}} + \mathbf{B}_\psi^{fc}\, \mathbf{d\tilde{w}}_\psi^c\ , \tag{82i}$$

$$\mathbf{d\tilde{w}}_\psi^c = -\boldsymbol{\beta}_\psi\, \tilde{\mathbf{w}}_\psi^c\, dt + \mathbf{dw}_\psi^c\ . \tag{82j}$$

$$\text{with}\quad \tilde{\mathbf{w}}_\psi^c(0) \sim (\mathbf{0}, \boldsymbol{\Sigma}_\psi)\quad \text{and}\quad \mathbf{w}_\psi^c \sim (\mathbf{0}, 2\boldsymbol{\beta}_\psi \boldsymbol{\Sigma}_\psi)\ .$$

Evolution of Uncertainties:
Predicted Standard Deviation of Temperature Error at 10m

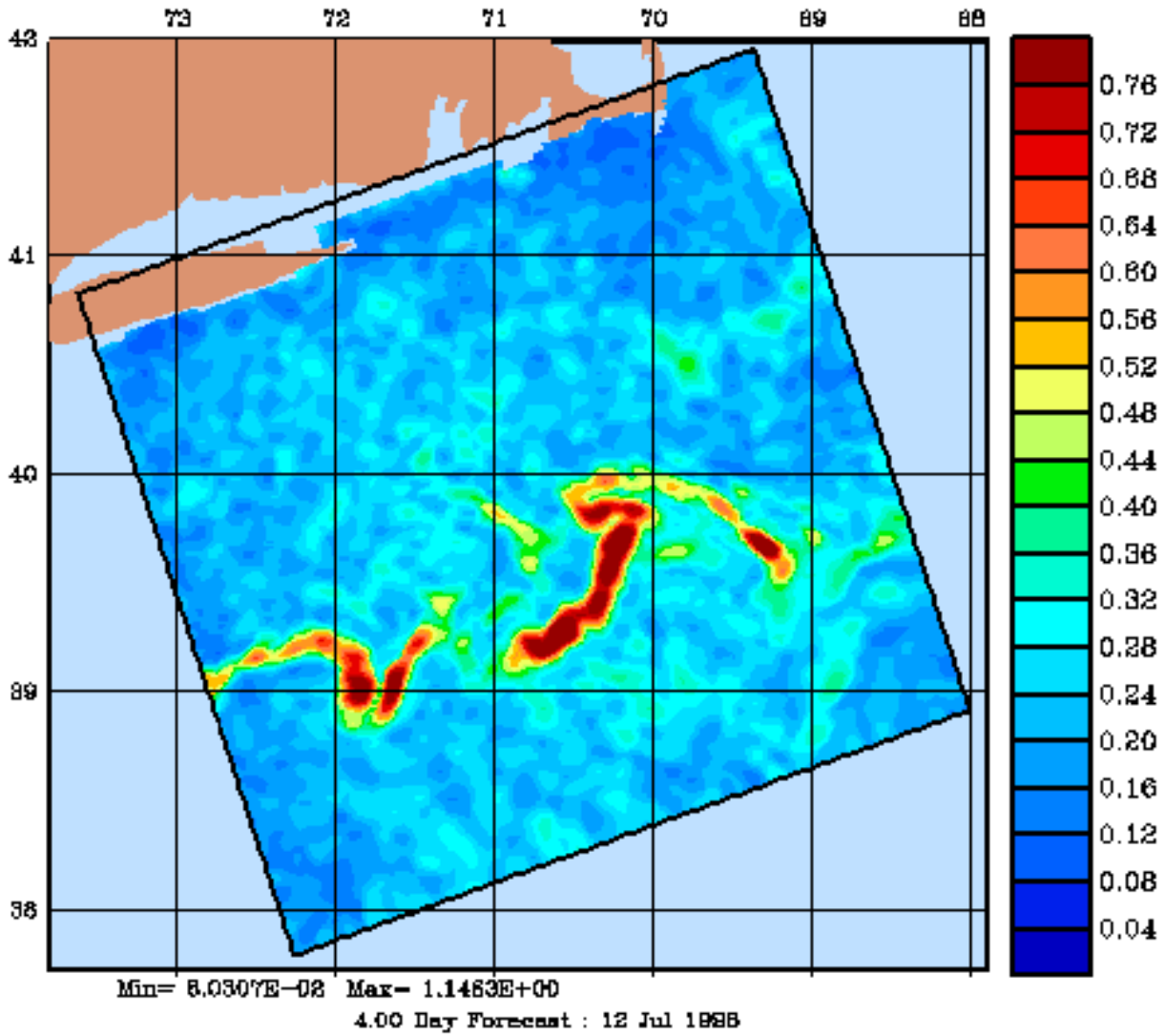

Acoustic Propagation Parameter: HOPS sound-sections at noon time

HOPS sections: 3 km grid (6-10 km scale)

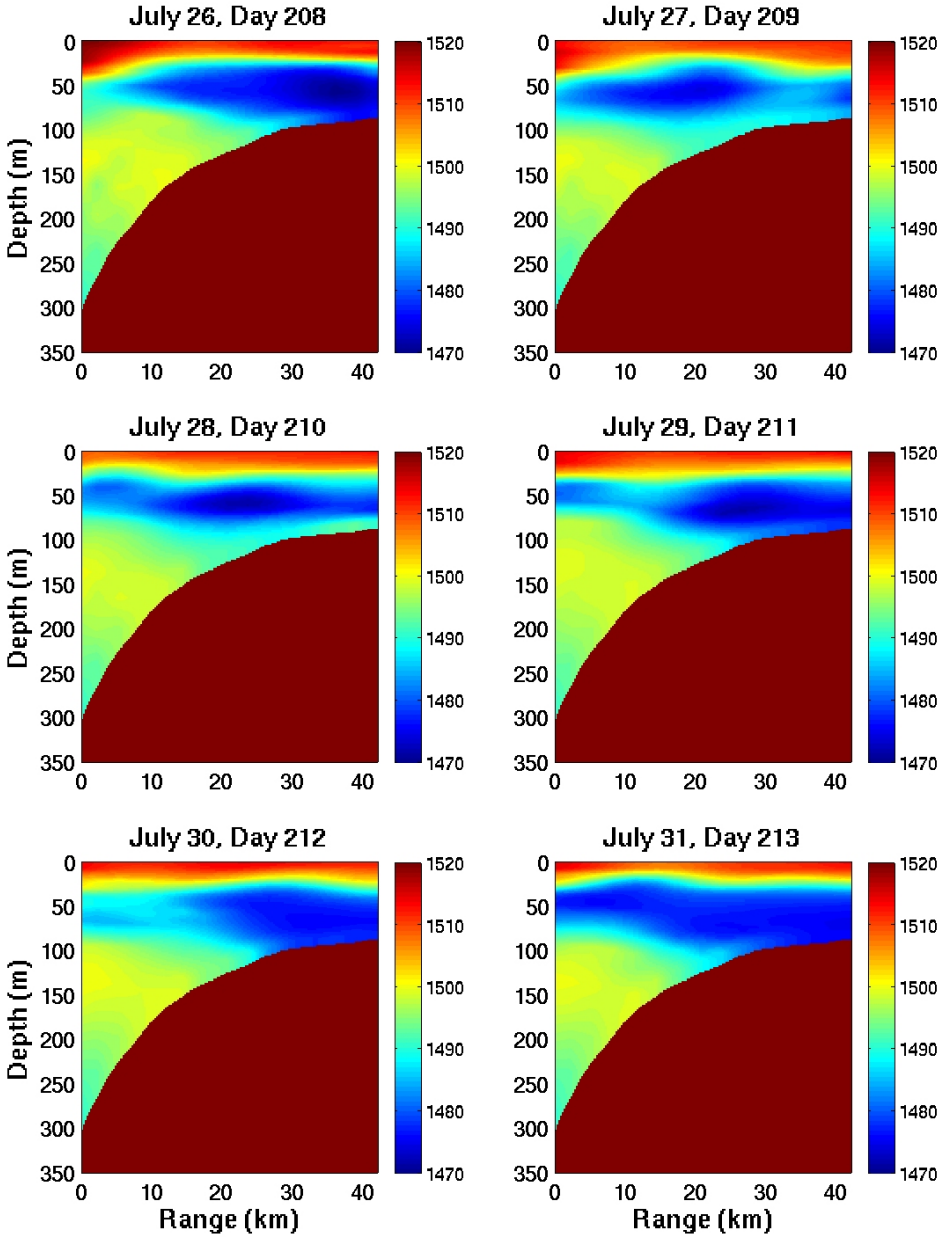

Seasoar + moored data (4 km cor. scale)

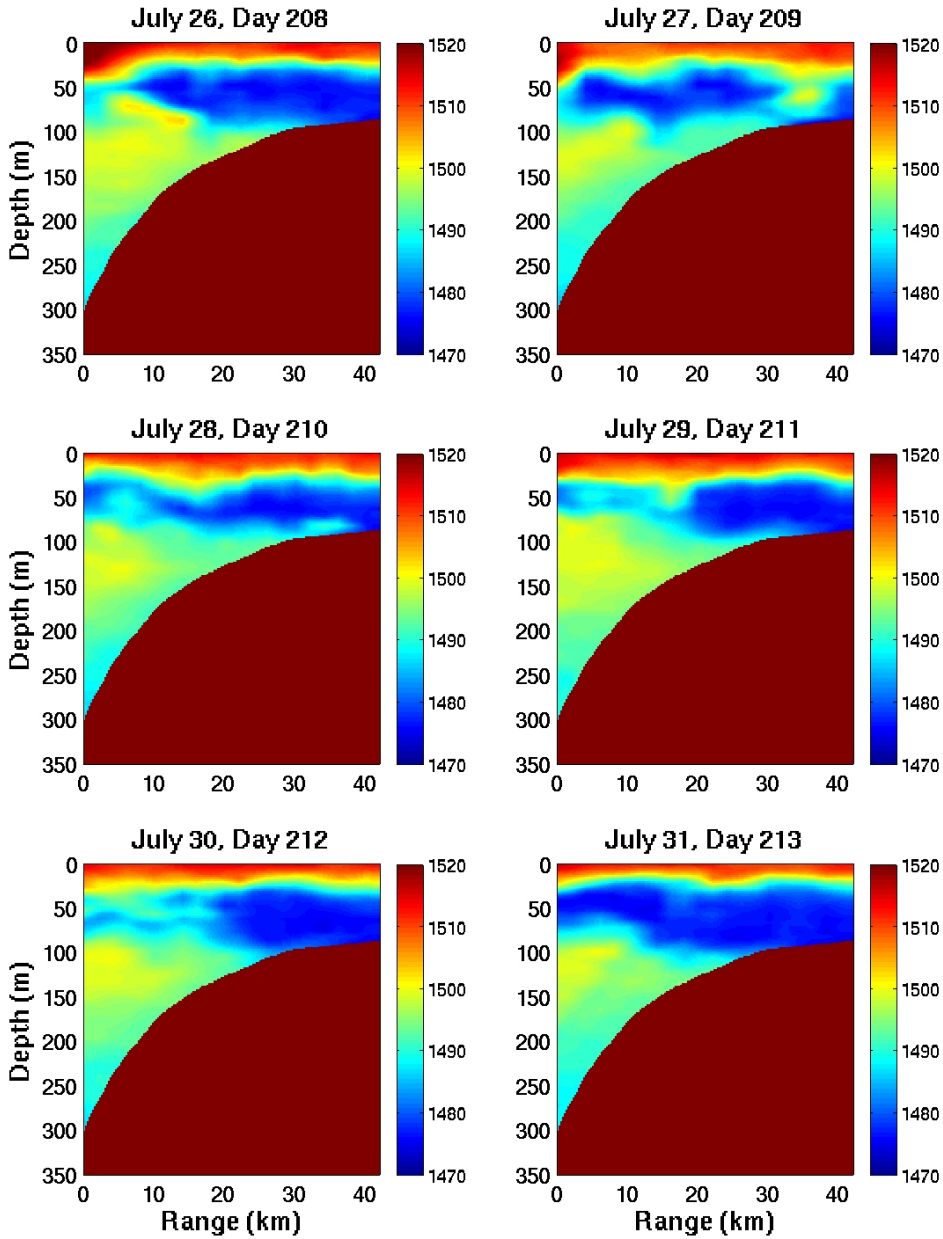

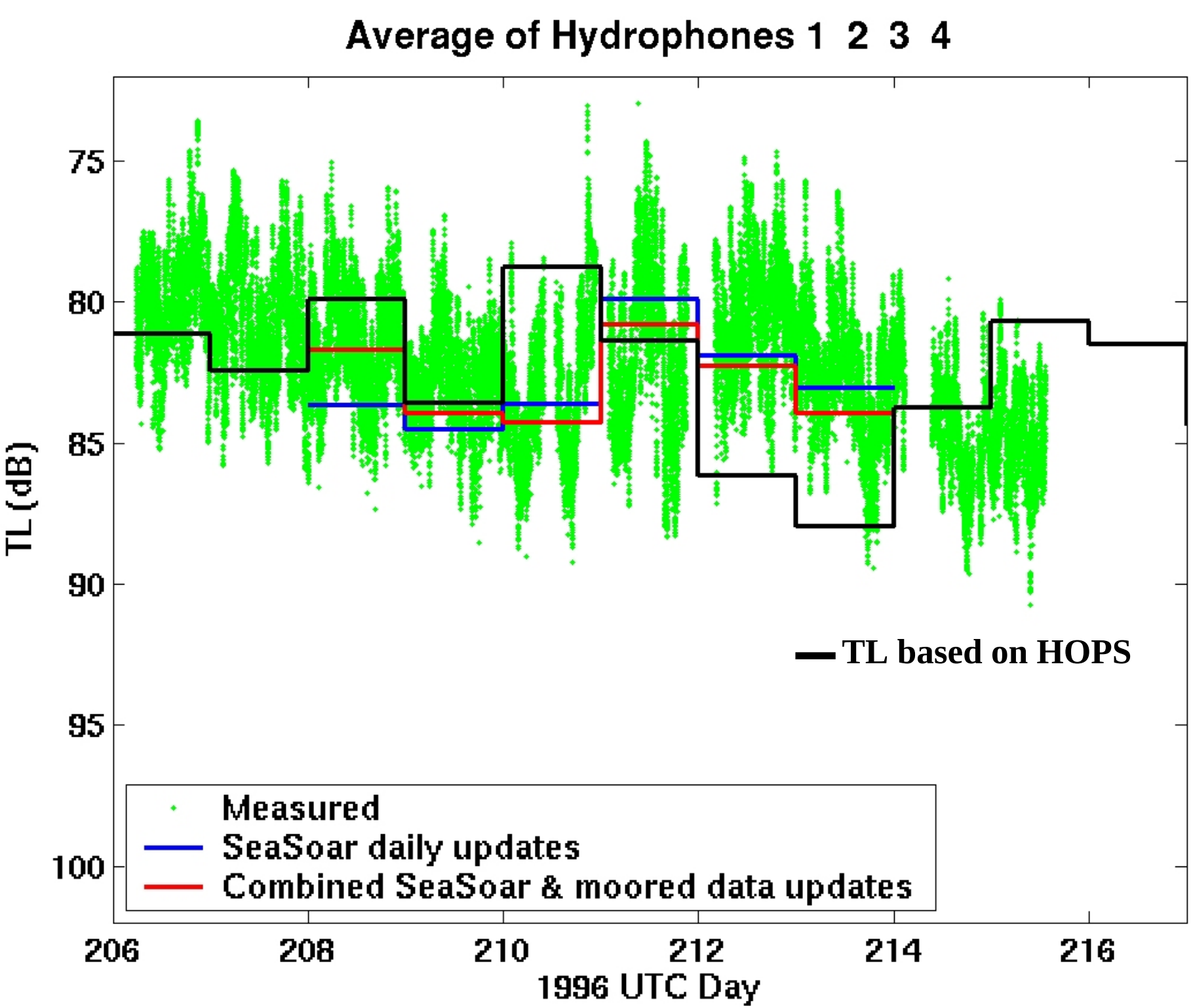
Average of Hydrophones 1 2 3 4
TL (dB)
75
80
85
90
95
100
206
208
210
212
214
216
1996 UTC Day
TL based on HOPS
Measured
SeaSoar daily updates
Combined SeaSoar & moored data updates

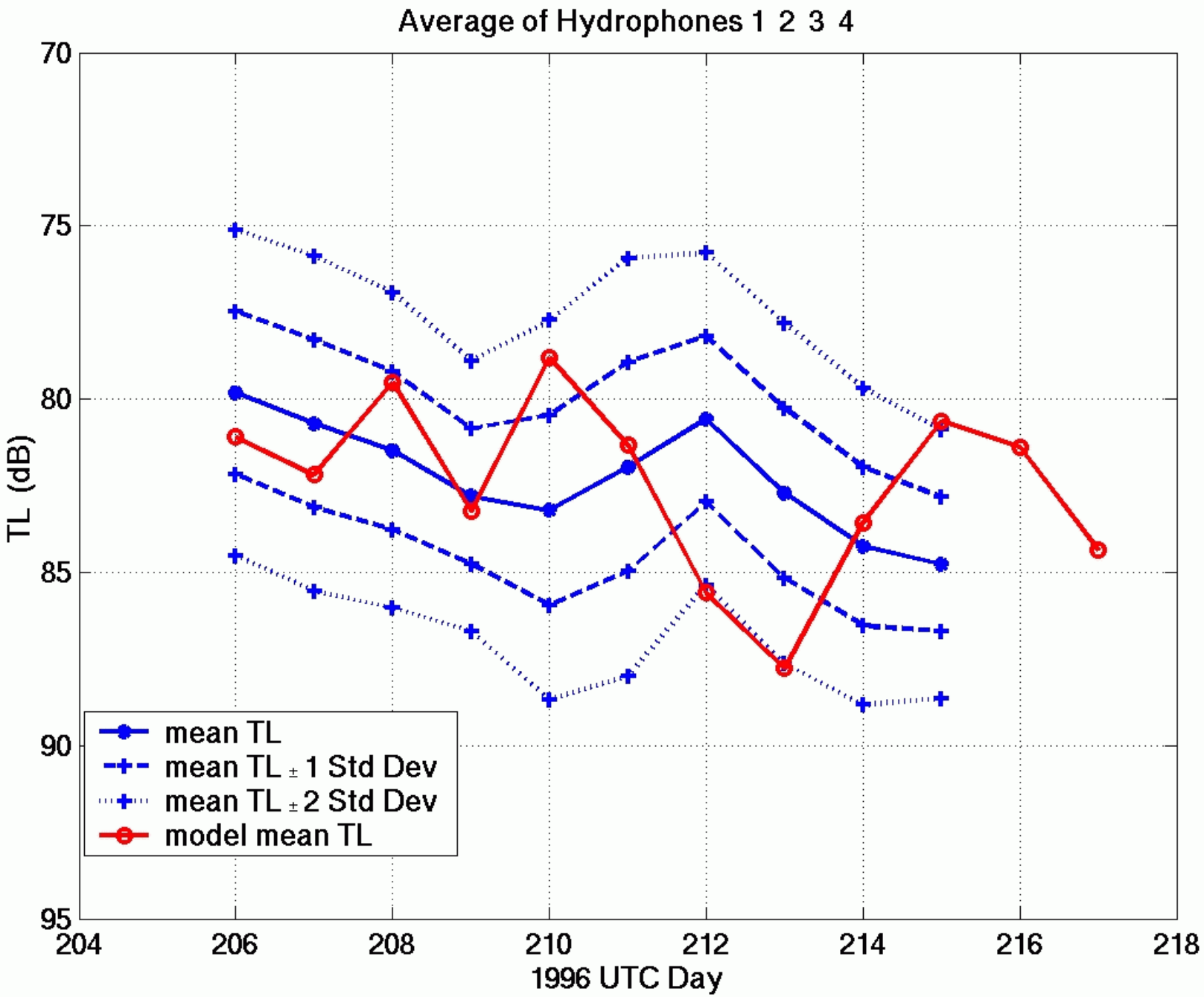
Average of Hydrophones 1 2 3 4
70
75
80
85
90
95
TL (dB)
204
206
208
210
212
214
216
218
1996 UTC Day
mean TL
mean TL ± 1 Std Dev
mean TL ± 2 Std Dev
model mean TL

Coupled Physical-Acoustical Data Assimilation of real TL data: Eigenmodes of coupled normalized error covariance on Jul 26

Sound-speed Component

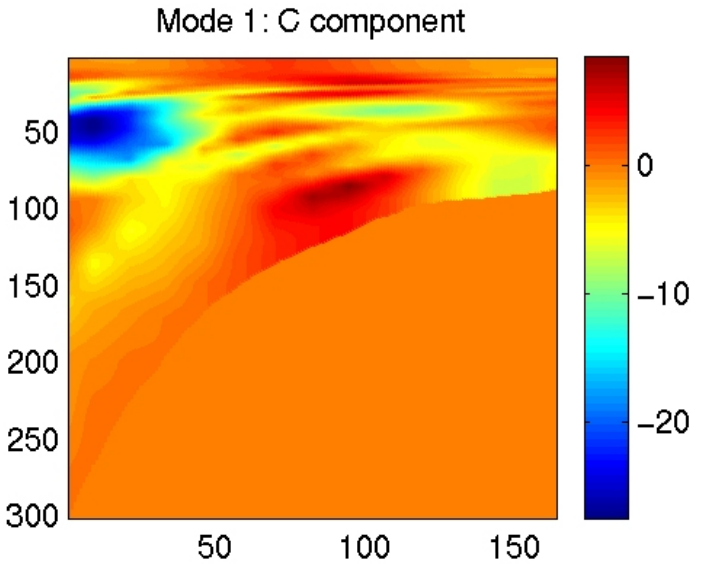

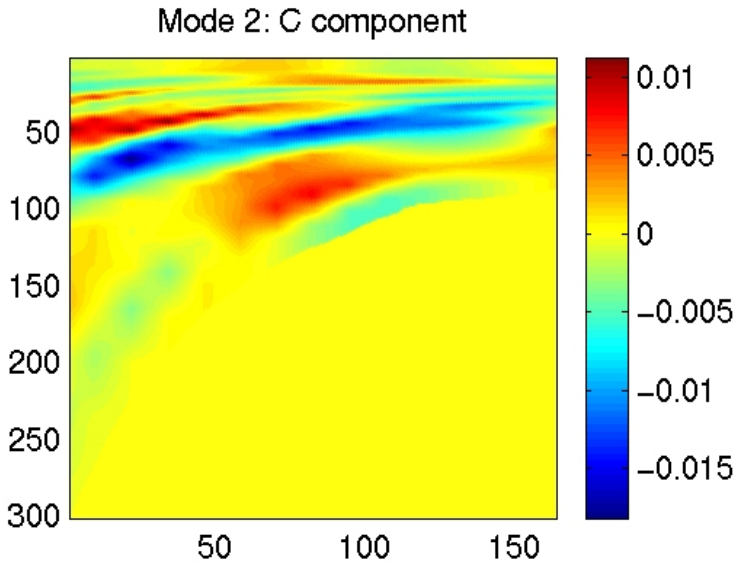

Broadband TL Component

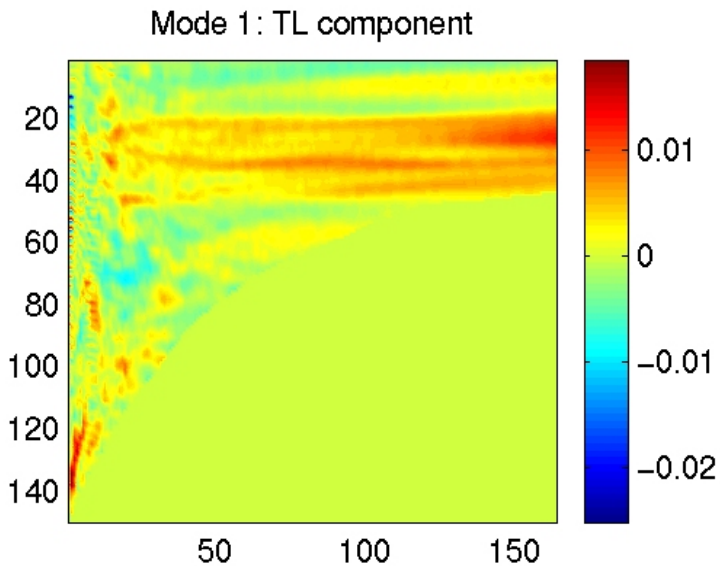

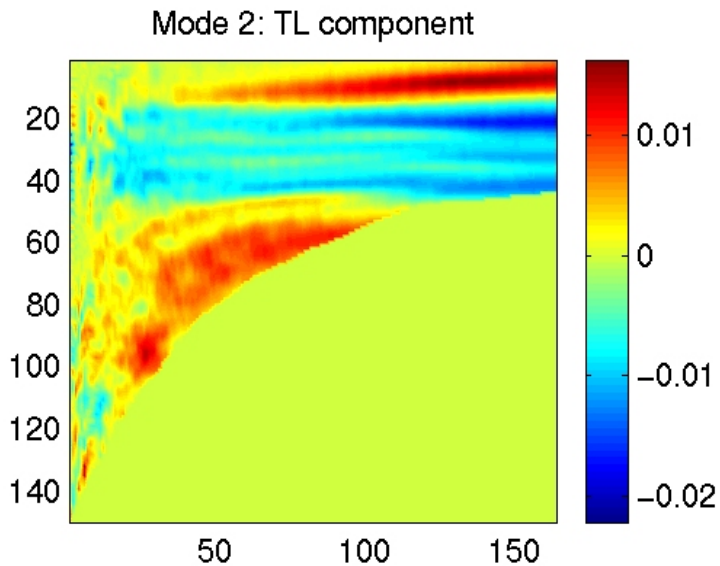

Shift in frontal shape (meander) and its acoustic TL counterpart above source and in cold channel

Opposition to mode 1 + surface thermocline tilt, leading to less (more) loss in cold channel (surface and bottom duct)

Coupled Physical-Acoustical Data Assimilation of real TL data

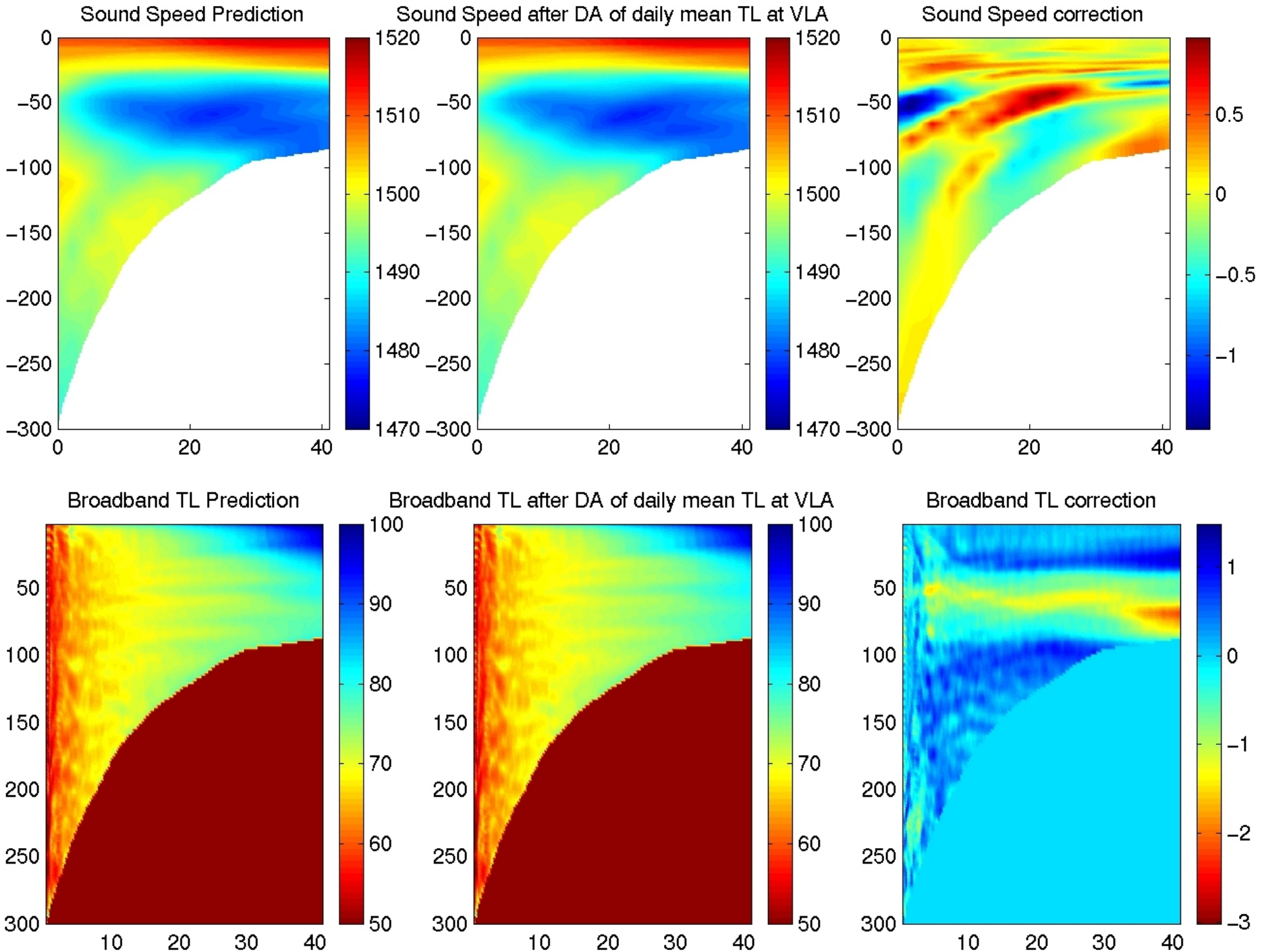

ASIAEX – April 2000

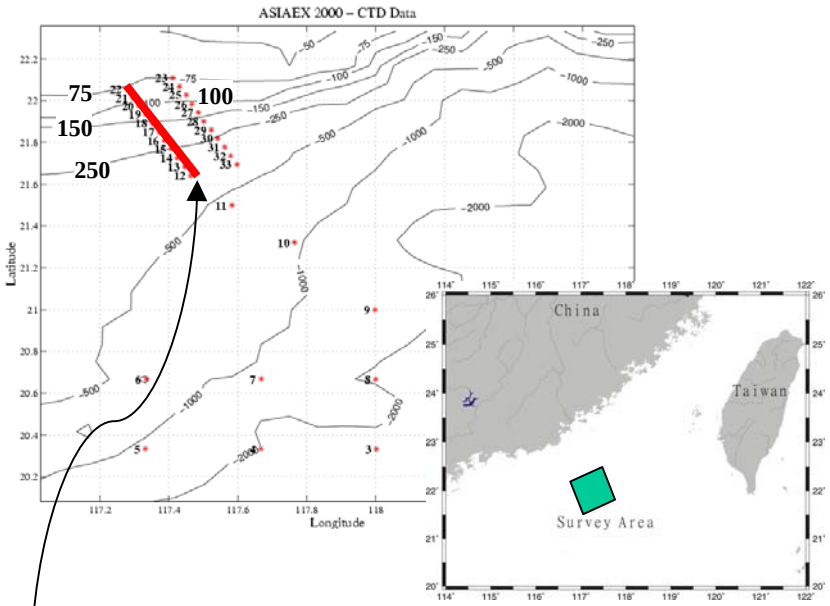

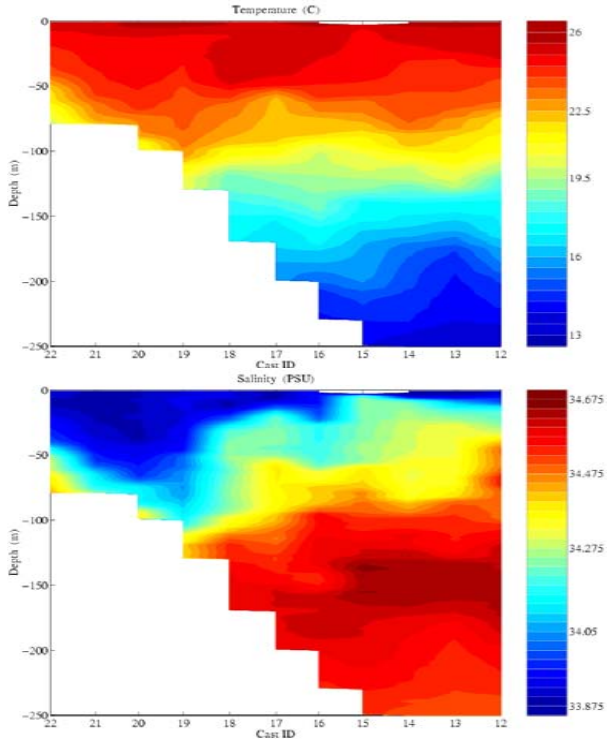

Temperature

NW-SE Section near 117.4E (~50km) 19 April 2000

Salinity

Section Locations

PRIMER – JUL/AUG 1996

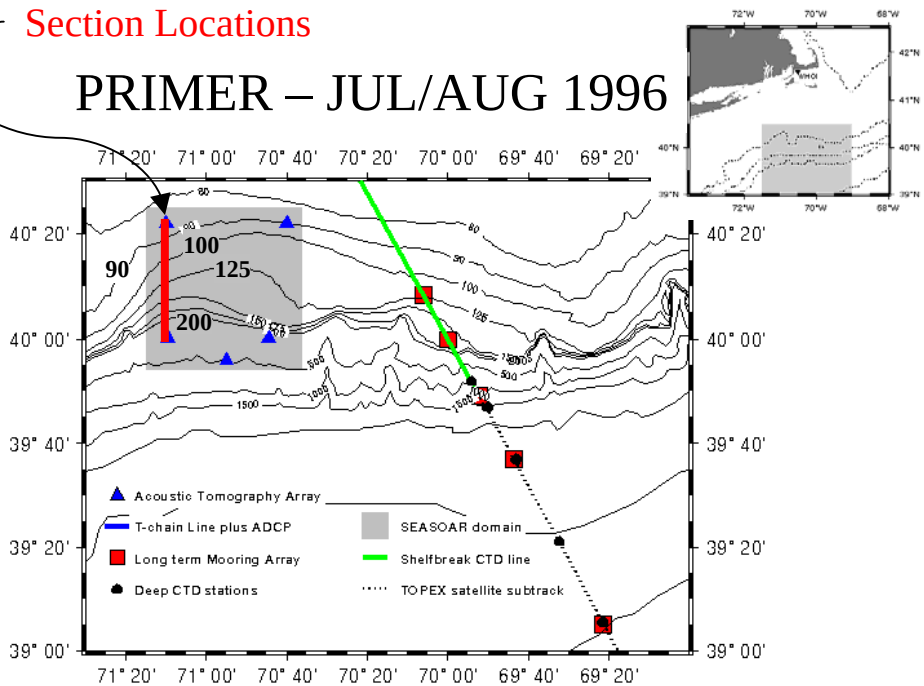

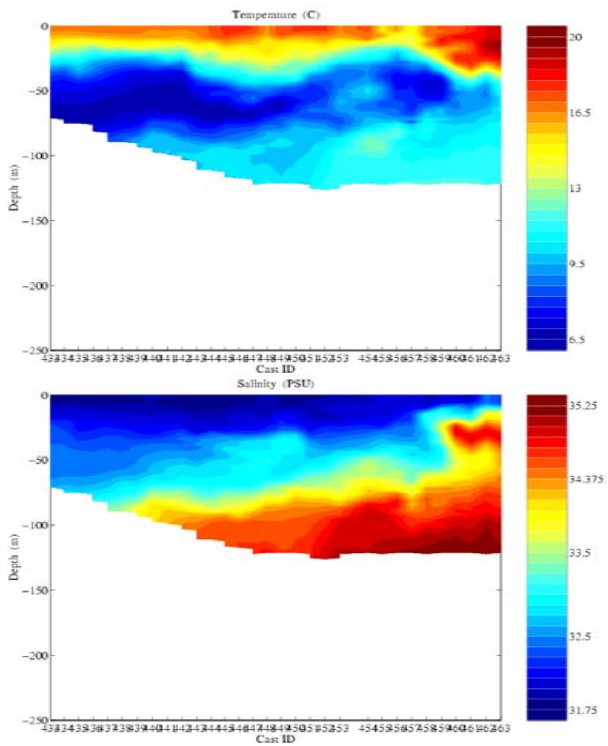

Temperature

N-S Section along 71.15W (~44km) 28 July 1996

Salinity

Comparison of PRIMER ’96 and ASIAEX ’00 Shelfbreak Fronts

	PRIMER	ASIAEX
Temp. Range of Section	6.5 – 20^{o}	13 – 26^{o}
Salinity Range of Section	31.75 – 35.25 PSU	33.875 – 34.675 PSU
Salinity Difference across Front	~1.625 PSU	~0.2 PSU
Slope	.0020	.0023
Width	5 – 10 km	5 – 20 km
Foot	100m	110m
Notable	Strong surface heating	Front not always present (e.g. 2001)

Ensemble statistics for ASIAEX 2000

30m Salinity; 15 members

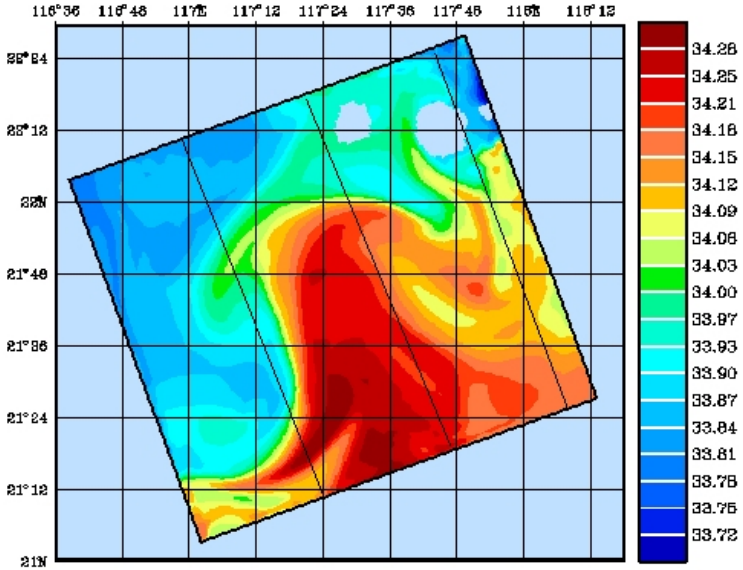

Mean

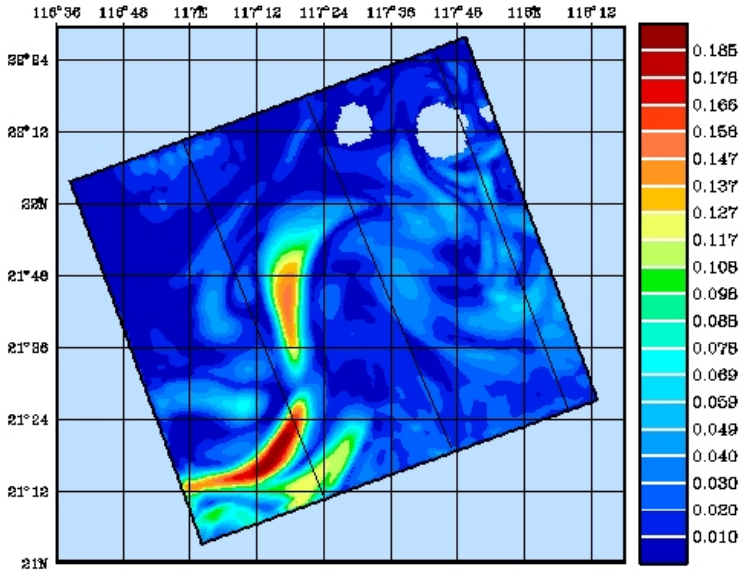

Standard Deviation

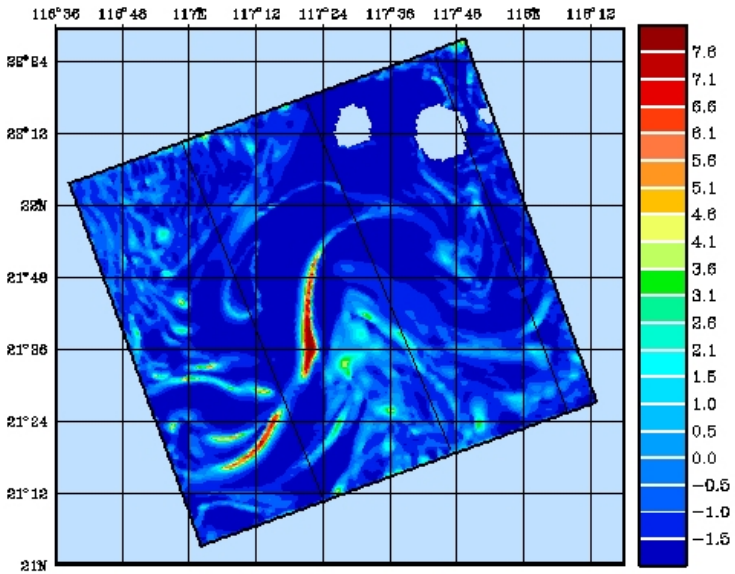

Kurtosis

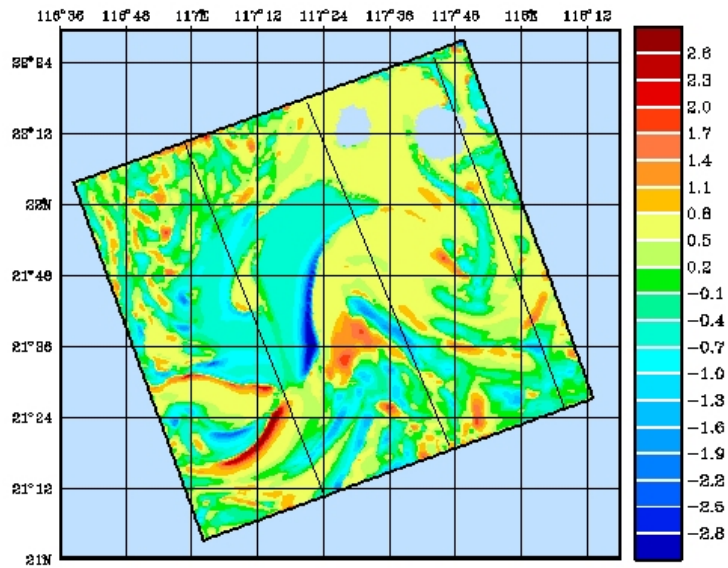

Skewness

Ensemble statistics for PRIMER 1996

Surface Sound Speed; 80 members

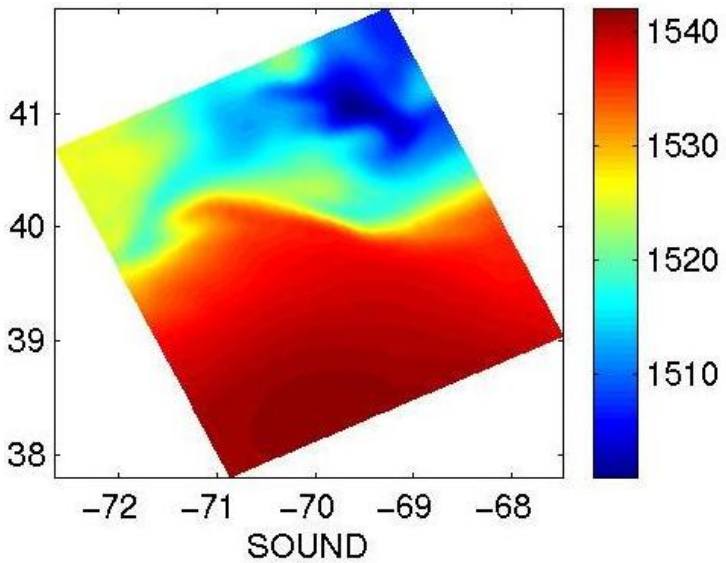

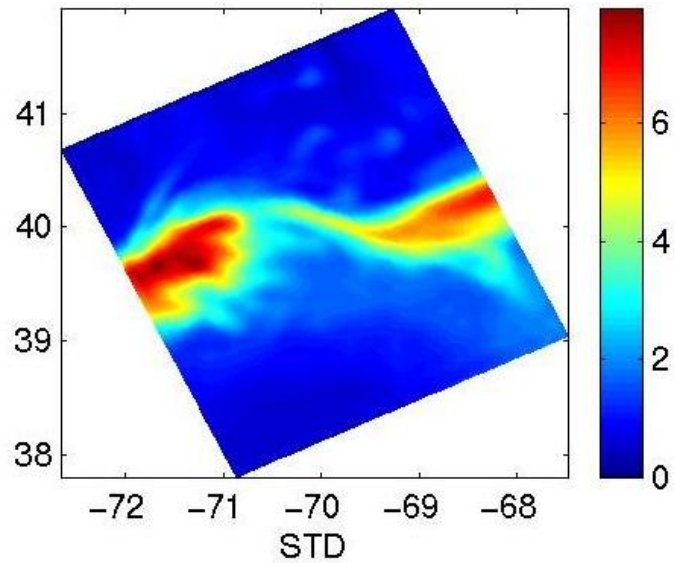

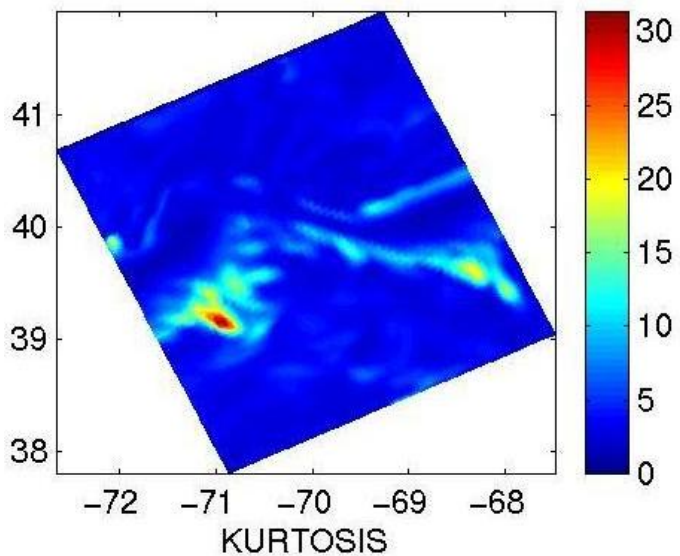

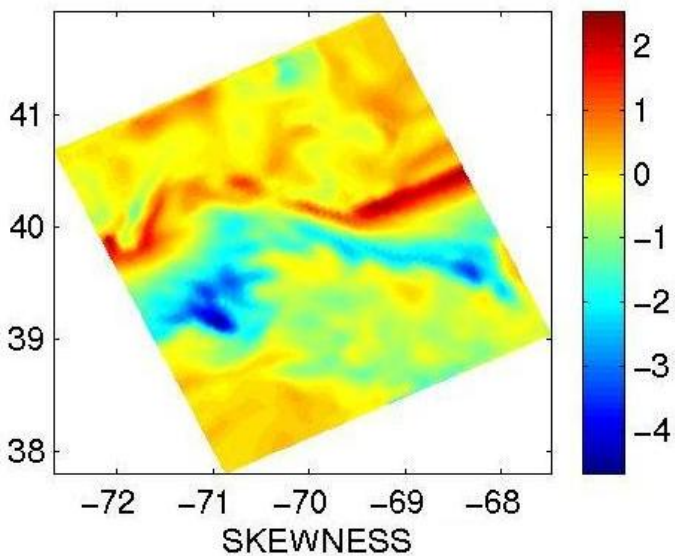

CONCLUSIONS

- Achieved 1-month simulation of ocean physics and its uncertainties at accuracy useful for acoustic propagation predictions
  - Ocean prediction acoustically useful even at times where there is no physical data
  - Requires steep topographies and intensive parameter estimation/fit, but is feasible today
- Shelfbreak PRIMER oceanic processes:
  - Large meander captured (prior to data assimilation). Arises due to a combination of internal ocean instabilities and atmospheric forcing
  - (Sub)-mesoscale eddy field at the front important in summer conditions and similar to open ocean eddies
- Most multiple sources of physical uncertainties accounted and predicted using dominant error approach of ESSE: non-stationary error statistics
- Oceans physics/acoustics data assimilation via ESSE: carried-out with real data as a single multi-scale joint estimation for the first time, using higher-moments to characterize uncertainties
  - Corrects too lossy TL at depth (2 db) and two high in surface mixed layer
  - Leads to corrections in whole acoustic section within cold channel and to shift in sound-speed front above the source (slope water meander/eddy)

EXTRA VUGRAFS

Temperature along Western Acoustic Track
8 July – 7 August 1996

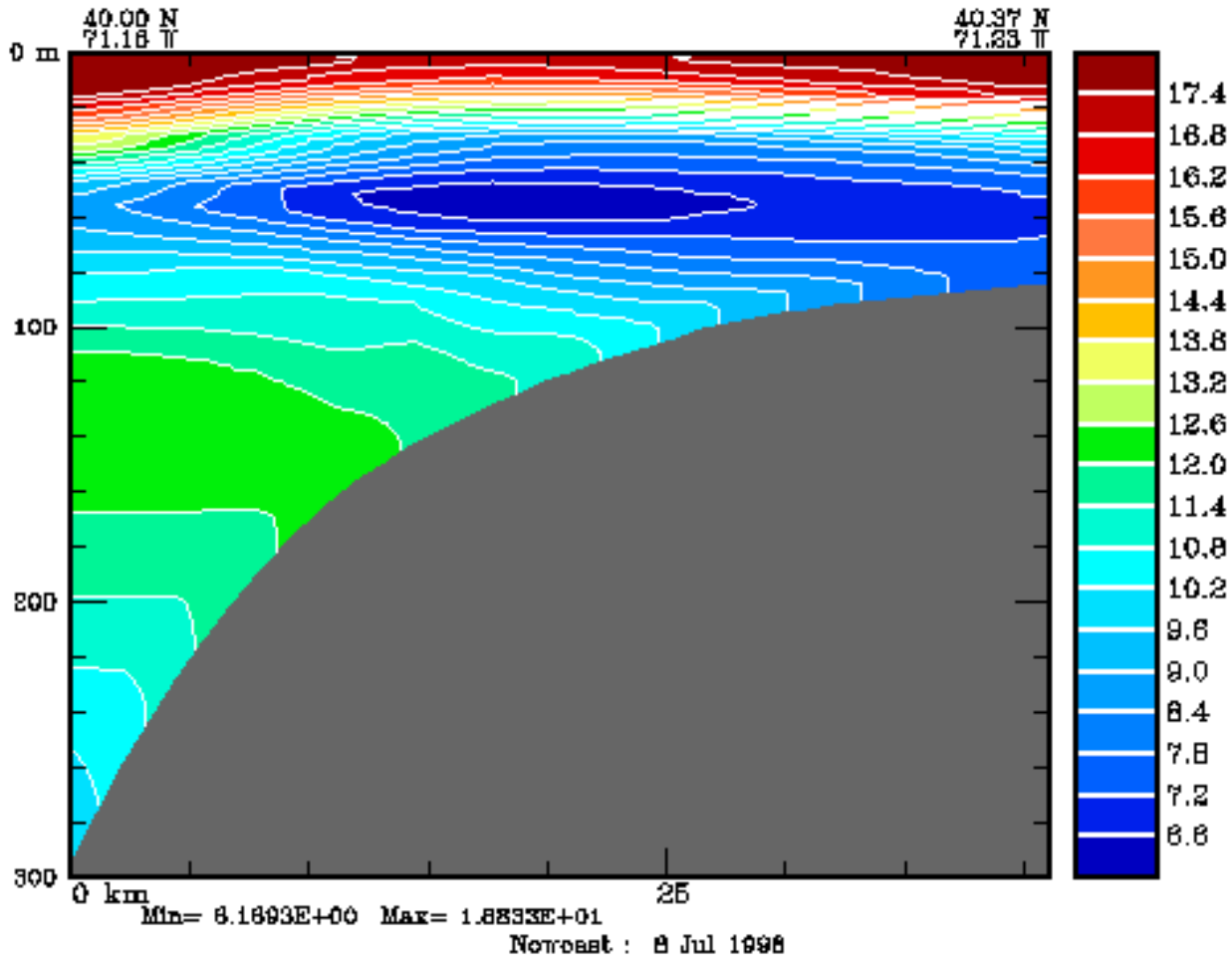

Case 13 (Conditioned): C=4.7, $\alpha = 0.04$

-73.4818 40.8695 **-72.1200 37.8340**

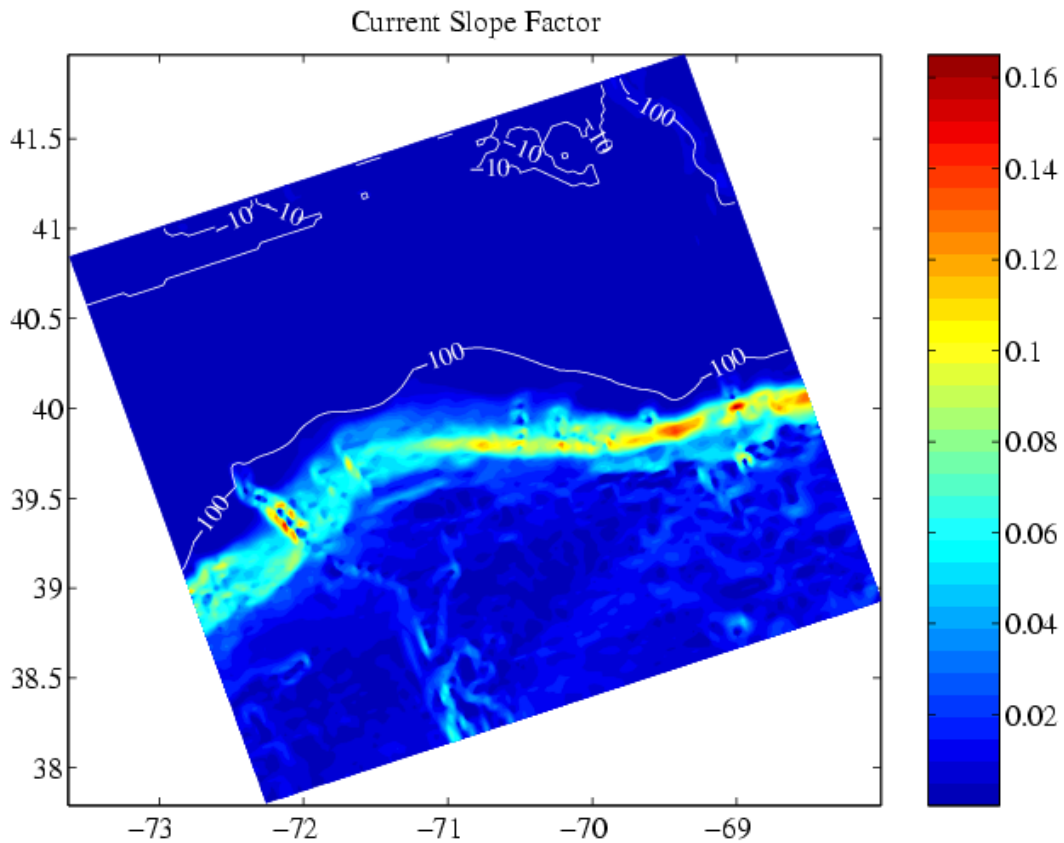

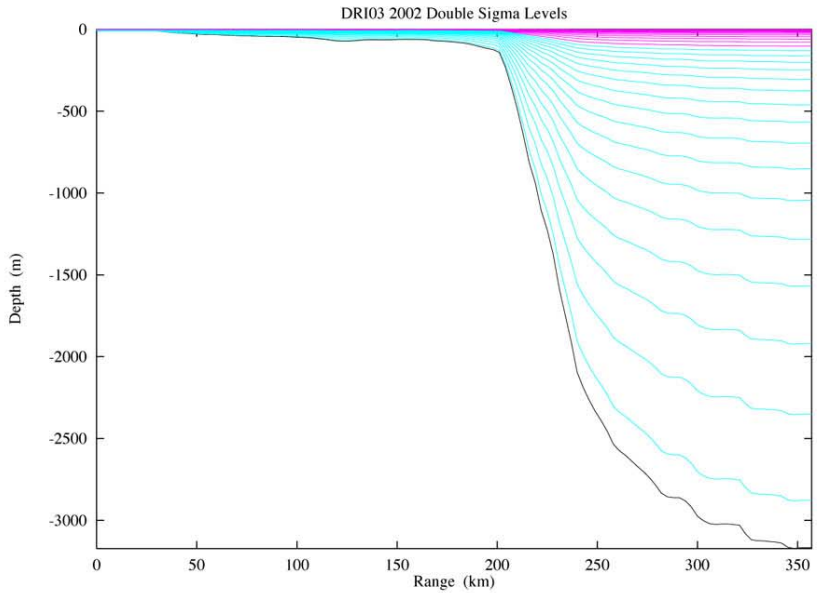

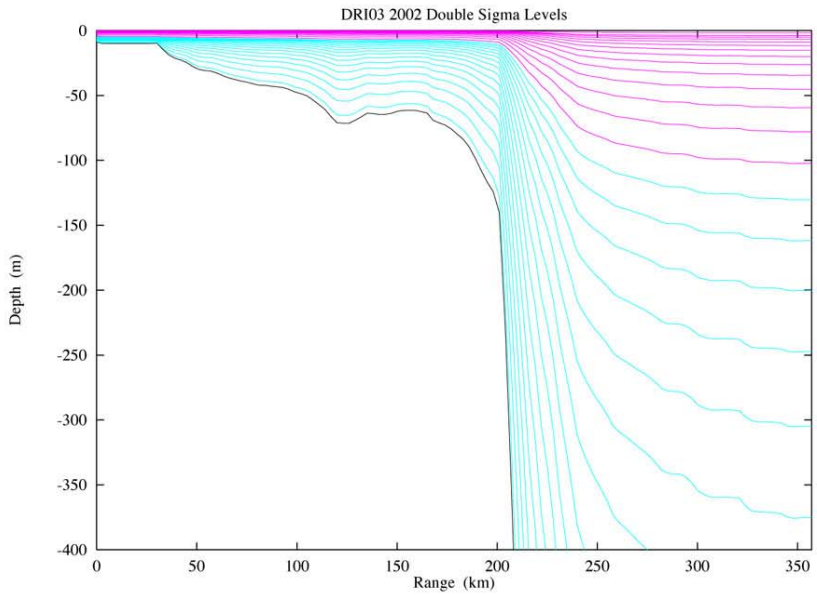

STOCHASTIC FORCINGS MODEL: Sub-grid-scales

I. 0d Random Noise Exponentially Decorrelated in Time

$$d\tilde{w} + \beta\,\tilde{w}\,dt = dw, \tag{76}$$

$$\dot{p}_{\tilde{w}} = -2\beta\,p_{\tilde{w}} + q\ . \tag{77}$$

Setting $\dot{p}_{\tilde{w}}$ to zero at all times yields $p_{\tilde{w}}(0) = \sigma^2 = \frac{q}{2\beta}$. The process $\tilde{w}$ is assumed to be of fixed fluctuation amplitude σ and autocorrelation time $\frac{1}{\beta}$. The constant variance of the white noise w is thus set to $q = 2\beta\sigma^2$.

II. 3d Random Noise, Exponentially Decorrelated in Time and 2-Grid Point Decorrelated in Space

$$\mathbf{d}\boldsymbol{\psi}^t = \mathbf{f}^{PE}\big(\boldsymbol{\psi}^t, t\big)\ dt + \mathbf{B}^{fc}(t)\ \mathbf{d}\tilde{\mathbf{w}}^c\ . \tag{86a}$$

$$\mathbf{d}\tilde{\mathbf{w}}^c = -\boldsymbol{\beta}^c \tilde{\mathbf{w}}^c\, dt + \mathbf{dw}^c\ , \tag{86b}$$

where symbols denote the:

- **discrete-space PE state vector:** $\boldsymbol{\psi} = (\hat{\mathbf{u}}, \hat{\mathbf{v}}, \mathbf{T}, \mathbf{S}, \mathbf{p})^T \in \mathbb{R}^n$
- **coarse 3d white noise:** $\mathbf{w}_k^c$
- **Coarse 3d Gauss-Markov process:** $\tilde{\mathbf{w}}_k^c$**,**

  i.e. $\mathbf{dw}^c = (\mathbf{dw}_{\hat{u}}^c, \mathbf{dw}_{\hat{v}}^c, \mathbf{dw}_T^c, \mathbf{dw}_S^c, \mathbf{dw}_\psi^c)^T$
- **PE dynamical model operator:** $\mathbf{f}^{PE}\big(\cdot, t\big)$
- **linear extrapolation matrix, from coarse to fine state:** $\mathbf{B}^{fc}(t)$

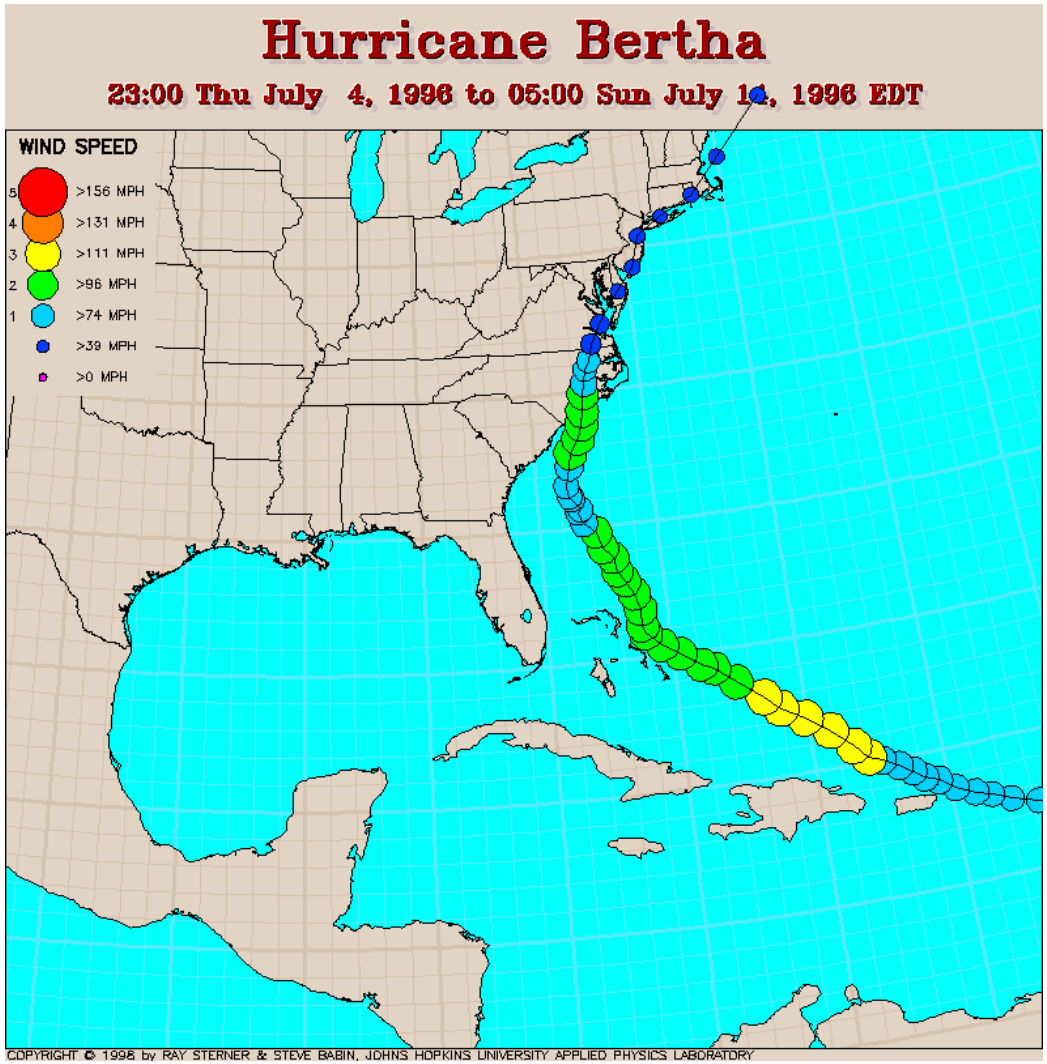

Averaged wind-stress time-series